NTNU – Trondheim
Norwegian University of
Science and Technology

Architecture and tectonic evolution of the Vøring and Møre rifted margins: insights from seismic interpretation combined with potential field modeling.

Iryna Podtykan

Geology

Supervisor: Stephen John Lippard, IGB
Co-supervisor: Gwenn Peron-Pindivic, NGU

Norwegian University of Science and Technology
Department of Geology and Mineral Resources Engineering

Abstract

The mid-Norwegian Vøring and Møre margins are listed as the type example of volcanic rifted margins, with their formation usually related to the influence of the Icelandic plume. Recent studies have shown that these margins have more in common with non-volcanic rifted margins than the scientific community used to think, which opens the discussion on their architecture and evolution. As the rifting mechanisms are not yet fully constrained, a wide variety of extensional models have been proposed in the literature. The evolution of the rifting models requires updated studies based on the new concepts and the new high resolution datasets now available.

Despite the large amount of geophysical data acquired on the Vøring and Møre margins during the past decades, the ambiguity with respect to the deep structures, and especially in detecting sub-basaltic basement structures, where intrusions and lava flows perturb the seismic imaging, is still a matter of concern.

This study illustrates the benefit of the combination of seismic and potential field modeling results. The forward gravity and magnetic modeling significantly improves the model accuracy and provides a valuable tool to estimate sub-basaltic deep crustal structures.

Acknowledgements

The Geological Survey of Norway (NGU) in cooperation with the Department of Geology and Mineral Resources Engineering at NTNU initially gave me this Master thesis. Professor Stephen J. Lippard from NTNU offered me the thesis and had the main input on the initial stage.

I would like to take an opportunity to thank the following contributors making the thesis possible.

First of all, I would like to thank my supervisor Gwenn Peron-Pindivic for her guidance and help during the project. I am grateful for her ideas and input during the project, and taking the time to answer all my questions during her maternity leave.

I wish to express my gratitude to the Team leader of the Continental Shelf Geophysics at the Geological Survey of Norway Odleiv Olesen for providing working facilities and giving me the opportunity to use a compilation of gravity and magnetic data from NGU. I want also to thank Jorg Ebbing from NGU for helping me with gravity and magnetic modeling.

Thank also to Professor Stephen J. Lippard (NTNU) for corrections and comments on my drafts.

I also wish to thank Martin, the loved one, for his support.

Contents

1 Introduction

1.1 Background

Decades of investigations of lithospheric extension led to the early definition of two classes of rifting: active and passive. In active rifting, deformation is commonly supposed to be associated with a mantle plume activity at the base of the lithosphere. The driving mechanism responsible for the extensional tectonics at the margin is heat transfer from the plume and magma generation. On the contrary, passive rifting involves mechanical stretching of the continental lithosphere, as a 'passive' response to regional tensile stress (Fig.1.1). The related 'passive' margins are characterized by seaward thickening prisms of marine sediments overlying stretched continental lithosphere. In theory, passive margins are characterized by normal heat flow and are dominated by gravity-driven collapse, halokinesis and growth faulting [Allen and Allen, 2005]. The margins surrounding the Atlantic Ocean are listed as typical passive margins.

Passive margins are furthermore subdivided into volcanic and non-volcanic margins. Volcanic (magma-dominated) margins are characterized by thick igneous crust with underplated material, while non-volcanic (magma-poor) margins are supposed to be devoid of any significant magmatic material (Fig.1.2).

Recent studies began to cast doubt on these classical definitions and proposed that the formation and evolution of 'passive' margins are more complex than previously assumed and that the similarities and differences between 'volcanic' and non-volcanic' margins are more subtle than a two end-member scenario (for a review see Peron-Pindivic et al. [in press]). Rifting models were mainly based on the study of the proximal domains of rifted margins, where data acquisition was concentrated in sedimentary basins with hydrocarbon potential. As a consequence, little was known on the distal domains. The datasets were biased and models developed onshore in continental rifts or offshore in proximal settings used to be applied directly to the overall margins, what resulted in oversimplifications. The acquisition of higher-resolution geophysical data (seismic, potential field) combined with deep sea drilling and onshore analogue studies show that rifted margins are structurally different from what was assumed before. These results questioned the validity of existing rifting models and led to the development of new concepts and approaches, mainly based on the study of key areas like the Iberia-Newfoundland conjugates, the North-East and South Atlantic systems.

The mid-Norwegian Vøring and Møre margins are usually listed as the type example of volcanic rifted margins [Planke et al., 2000; Skogseid et al., 1992]. These have been affected by voluminious postrift magmatism, and their formation is regularly related to the influence of the Icelandic plume. However, recent studies cast doubt on this basic definition and proposed that they have much in common with magma-poor margins, what opens the discussion on the proper architecture and evolution of the margins [Osmundsen et al., 2002; Osmundsen and Ebbing, 2008; Peron-Pindivic et al., in press].

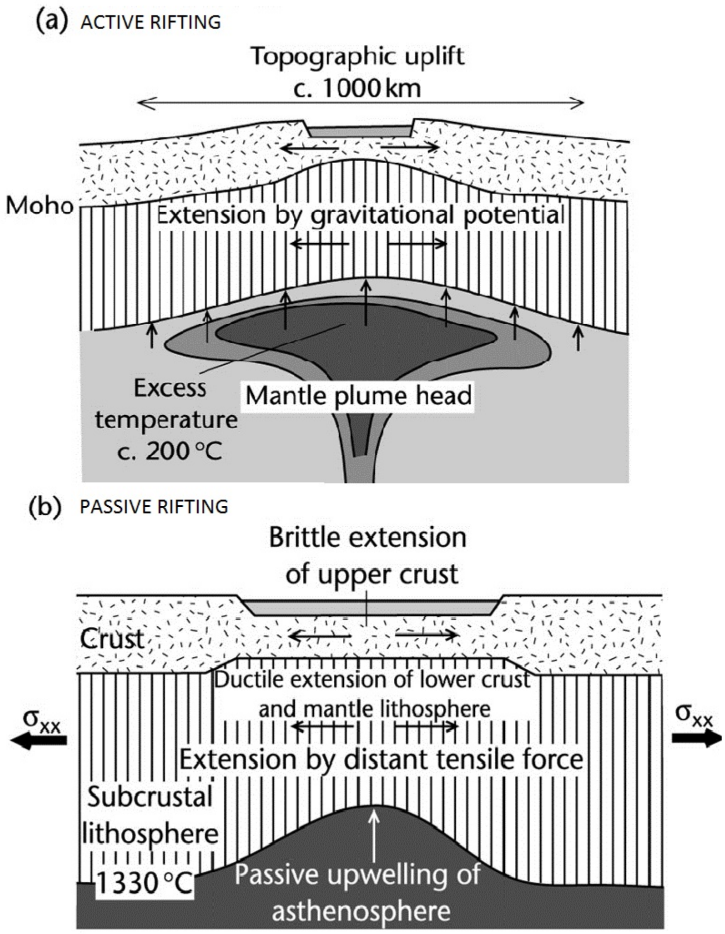

Figure 1.1: Two classes of rifting: a) active rifting with deformation as a consequence of mantle plume activity; b) passive rifting with stretching of the lithosphere, as a 'passive' response to regional tensile stress. From Allen and Allen [2005].

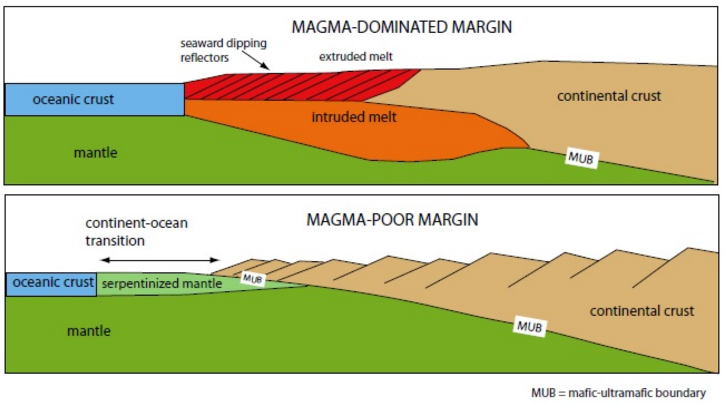

Figure 1.2: Two types of margin: a) volcanic or magma-dominated margin with thick igneous crust and underplated material; b) non-volcanic or magma-poor margin with no magmatic material. Modified from Sawyer et al. [2007].

1.2 Organization of the thesis

The study presented in this thesis begins with literature summary, in order to propose an overview of the evolution of the extensional models published in the literature.

The 'Tectonic Setting' chapter gives the overview of the geological evolution and structural setting of the Norwegian Sea Continental Margin, with the emphasis on the Vøring and Møre Margins. This chapter includes the development of the NE Atlantic as a whole with focus on the main tectonic periods, followed by a closer insight into the study area and structural settings of the Vøring and Møre basins.

The 'Dataset' chapter gives an overview of the seismic (reflection and refraction), gravity and magnetic data which have been used in the study. The 'Methodology' chapter then outlines the project main workflow with introduction of the software programs used in the thesis.

The chapter 'Results and discussion' is presented to give a more detailed description of each step of the workflow. The Seismic Interpretation part is based on the structural and depositional history of the studied area, and is subdivided into the main structural features part (from Seabed down to the BCU) and the deeper crustal levels part (from BCU further down into the deeper interfaces). The Depth Conversion part further presents the conversion of two-way time (twt) sections to geological depth sections. The Potential Field Modeling part is intended to revise the model by doing forward modeling of the crustal structure of the margin. The forward model calculation is divided into three steps. First, a simple model constructed on the available depth converted seismic data. Second, the gravity and magnetic signal are calculated and compared with the observed anomalies. Finally, the model is improved further in order to better fit the observed and calculated gravity and magnetic anomalies. Considering a wide variety of extensional models and different interpretations of the Vøring and Møre margins, the nature of the marginal high, the basement, the oceanic crust, the continent-ocean transition (COT), the lower crustal body (LCB) and the mantle have been discussed. The final model was carried out by interactive changes in the geometry and properties of the layers and is based on the seismic data (reflection and refraction), gravity and magnetic measurements, and published investigations.

Finally, conclusion is given in the last chapter.

2 Literature summary

It is now generally agreed that rifted margins form through continental rifting and break-up, however these mechanisms are not yet fully constrained. The rifting evolution can lead to various architectures [Ruppel, 1995] depending on the influence of several parameters (the extensional modes and rates, the continental lithosphere and underlying asthenosphere thermal structures, the rheology of the different lithospheric layers and the pre-rift mechanical conditions [Buck, 1991]). As a consequence, numerous rifting models have been proposed. Even if they evolved in parallel with developments in data acquisition and processing, the models are still dominated by two archetypes proposed quite early: the pure shear model of McKenzie [1978] and the simple shear model of Wernicke [1985] (Fig.2.1).

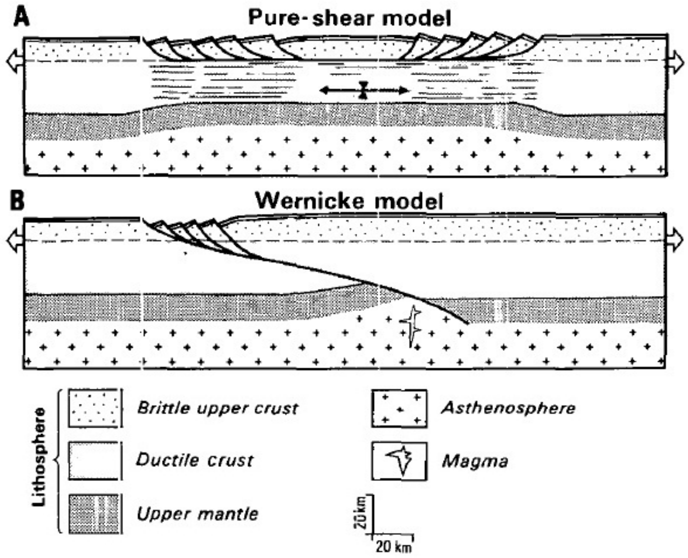

Figure 2.1: Two first key models of continental extension: A) symmetric extension pure-shear model of McKenzie with the brittle upper crust extended over the stretched ductile lower crust; B) asymmetric simple-shear model of Wernicke with a low angle detachment fault cutting through the entire lithosphere. Modified from Lister et al. [1986].

2.1 The first key models

The pure shear model of McKenzie [1978] proposes that deformation is uniformly distributed ($\beta_{crust} = \beta_{mantle}$), instantaneous, with no magmatic activity, radiogenic heat production and uniform temperature at the base of the lithosphere. The model explains the lithospheric extension leading to the development of symmetrical margins with rotated tilted blocks in the brittle crust, overlying the uniformly stretched ductile lower crust (Fig.2.1A). The model also assumes that the lithosphere stretching is uniform with depth and neglects the role of basement faults. Le Pichon and Sibuet [1981] applied this model to the formation of rifted margins. Despite the scarcity of quality data at that time, the available geophysical observations already cast doubt on the validity of the model to explain deep margin evolution. Numerous reflection profiles from various worldwide extensional environment did already show the importance of major basement faults cutting from the upper crust to the mid-lower crust during the formation of rifted basins [Kusznir and Ziegler, 1992]. As well, the studies revealed that the conjugate Iberia-Newfoundland margins are for instance rather asymmetric and that there are differences between the observed and calculated subsidences. Additionally, in the early 80's, Boilot et al. [1980] proved that part of the distal Iberia domain is formed by serpentinized exhumed mantle, what is incompatible with the pure shear model.

Meanwhile, in conjunction with the development of the detachment fault concept in the Basin and Range region to explain the formation of metamorphic core complexes [Davis, 1980],Wernicke [1985] proposed the simple shear model. His model suggests an asymmetric non-uniform stretching ($\beta_{crust} \neq \beta_{mantle}$), controlled by large scale detachment faulting with initiation angle in range of 10-30°. Low-angle normal faults cut the entire lithosphere (Fig.2.1B). Various authors extrapolated with success this model to rifted margins [Lister et al., 1986, 1991; Boilot et al., 1980, 1987b; Reston et al., 1996] or to fossil Tethysian margins in the Alps [Lemoine et al., 1987; Froitzheim and Manatschal, 1996]. However, as revealed by the acquisition of drilling and new geophysical data, this model does still not fully explain the overall evolution of continental rifting. It cannot provide a satisfactory explanation for the commonly observed partitioning of rifted margins into distinct domains of deformation (proximal and distal).

2.2 The application to rifted margins

Further developments of lithosphere stretching models have been proposed by Lister et al. [1986, 1991]. They adapted the simple shear model to margins and suggested the existence of upper- and lower-plate passive margins. The alternative scenario of this model involves the delamination of the lithosphere with the detachment zone below the brittle-ductile transition and/or at the crust-mantle boundary. The upper- and lower-plate margins differ in the rift-stage structure and uplift/subsidence characteristics. Passive margin can change along its length from an upper- to a lower-plate margin via transfer faults. An example of such pattern has been observed across the Jan Mayen Fault Complex (JMFC) which separates the Møre and Vøring Basins. Mosar et al. [2002] suggested the upper-plate geometry for the Vøring Basin and the lower-plate geometry for the Møre Basin. Lister et al. [1986, 1991] extensional model explains the asymmetry of non-volcanic margins, the existence of margin mountains, igneous underplating and the genesis of metamorphic core complexes.

2.3 The depth-dependent deformation

One of the key question concerning continental rifting is the distribution of deformation with depth. In the 80's, scenarios alternative to the McKenzie [1978] and Wernicke [1985] models began to discuss the importance of depth dependant deformation, following the partition of the lithosphere into upper brittle layers and ductile-plastic lower layers

[Jackson and McKenzie, 1983; Kusznir et al., 1987]. Davis and Kusznir [2004] notably showed that there is a mismatch between the thinning of the upper crust, the wholesale crustal thinning and the lithospheric thinning at rifted margins, and proposed a concept of depth-dependant extension. The variations in depth of the style, amount and timing of the extension are highly unconstrained and the subject of numerous debates [Ziegler, 1983; White et al., 1986; White, 1990]. Nagel and Buck [2004, 2007] and Huismans and Beaumont [2008, 2011] proposed that a pronounced decoupling of the deformation can occur between the upper mantle/lower crust and the upper crust, at the level of a weak zone in the lower crust.

On the contrary, Reston [2005, 2009] provided evidence for the polyphase faulting in order to explain the extension discrepancy. Based on observations from various magma-poor margins of the North and Central Atlantic, he suggested multiple phases of brittle deformation, related to changes in rheology of the lithosphere, and resulting in the extreme thinning of the crust. The rheological evolution of the lithosphere controls the transition from a decoupled to a coupled lithosphere with a related change from symmetric to asymmetric extensional tectonics.

2.4 The Iberia-Newfoundland contribution

The Iberia-Newfoundland system is unique in the sense that it is the only pair of conjugate rifted margins that has been drilled down to basement in several locations. 18 holes have been drilled during DSDP Leg 47B and ODP Legs 103, 149, 173 and 210 [Groupe-Galice, 1979; Boilot et al., 1987a; Sawyer et al., 1994; Whitmarsh et al., 1998; Tucholke et al., 2004]. The resulting data gave some new and crucial information on the basement lithologies and on the overall architecture, altogether permitting to further constrain and test the various rifting models.

The classical models were challenged by new data obtained from the deep margins. Whitmarsh et al. [2001] presented observations from the Iberia margin and fossil Alpine-Tethyan margin, and supported the existence of a zone of exhumed continental mantle (ZECM) between continental and oceanic crust. Considering the discovery of the ZECM, Whitmarsh et al. [2001] proposed a conceptual lithospheric scale model of rifted magma-poor margin development, which focuses mainly on the final stage of continental extension, break-up, and creation of the ZECM. The ZECM has distinctive geophysical and geological characteristics, different from those of typical continental and oceanic crusts: 1) the top-basement seismic velocity is lower than of the adjust continental crust, and the velocity in the lower layer is too high to represent the oceanic crust or underplated continental crust; on the other hand, the anomalous velocity structure reflects well the decreasing mantle serpentinization with depth; 2) the ZECM basement magnetizations are much lower than those of oceanic basement westwards, suggesting that the upper seismic layer contains little magnetic material, and the lower layer contains magmatic intrusions which increase in volume oceanwards, what would be coherent with an exhumed mantle more and more intruded by MORB material oceanwards.

The conceptual lithospheric-scale model exhibits the modes of extension from pure shear (symmetric rifting and decoupling of upper crust/upper mantle) to simple shear (with asymmetric rifting and coupling), and finally, to the sea-floor spreading phase with mantle exhumation and creation of the ZECM.

2.5 The recent multi-phase and multi-process models

Modifying the conceptual lithosphere-scale model, Manatschal [2004] focused particularly on the deformation processes related to rifting, in order to examine how the architecture of rifted margins is controlled by deformation, sedimentary, magmatic and hydrothermal processes. A major prediction is made that entirely non-magmatic margins do not exist. Manatschal [2004] provided the indirect evidence that crustal-scale faults thinned the crust to less than 10 km in an early stage of rifting. This model suggested three different fault systems responsible for the thinning of the lithosphere from the onset of rifting to final continental break-up, where the downward-concave faults controlled the final rifting leading to the mantle exhumation. The observed changes in basin architecture reflected the evolution of the bulk rheology of the lithosphere during extension.

Based on numerical experiments, Lavier and Manatschal [2006] proposed a numerical/conceptual/geological rift model with three rifting phases, with the evolution from a decoupled stretching phase to a final coupled exhumation phase. The mechanical decoupling of upper crustal deformation is achieved by a weakened ductile shear zone at mid-crustal levels. The transition from symmetric (stretching) to asymmetric stage (exhumation) is probably influenced by the gabbroic lower crust. The presence and the role of the gabbroic lower crust in the margin development is one of the key questions and still a matter of debate.

Based on the seismic and magnetic data, and on the ODP drilling results from the Iberia and Newfoundland margins, Peron-Pindivic et al. [2007] and Peron-Pindivic and Manatchal [2009] proposed to review the architecture of the deep Iberia-Newfoundland conjugate margins and their rifting evolution. The rifted margins are subdivided into distinct domains with the proximal domain, the necking zone, the (deep) distal domain including the OCT (ocean-continent transition (comprising the ZECM)), and the oceanic domain. Peron-Pindivic and Manatchal [2009] focused on key stages in the evolution of the margin: pre-breakup stage, stretching, thinning and exhumation stages. The authors proposed modification of the Lavier and Manatschal [2006] model, suggesting to add the modes that describe magma-controlled extension for a complete description of lithospheric rifting that leads to sea-floor spreading (Fig.2.2). Rifting is described as a polyphase process which cannot be explained by any model alone, but by the complex relationship between different modes. It was concluded that previous observations are not satisfactory enough for the explanation of crustal thinning to less than 10 km, and for the determination of continental breakup timing and location.

Similarly to the Iberia-Newfoundland system, the long-lived development of the NE Atlantic rift system is highly complex, which led to a wide variety of extensional models being proposed [Eldholm et al., 1989; Brekke, 2000; Scott et al., 2005; Osmundsen et al., 2002; Osmundsen and Ebbing, 2008]. The evolution of the extensional models from the first key models of McKenzie and Wernicke to the recent multi-phase and multi-process models requires updated studies based on these new concepts and the new high resolution datasets now available.

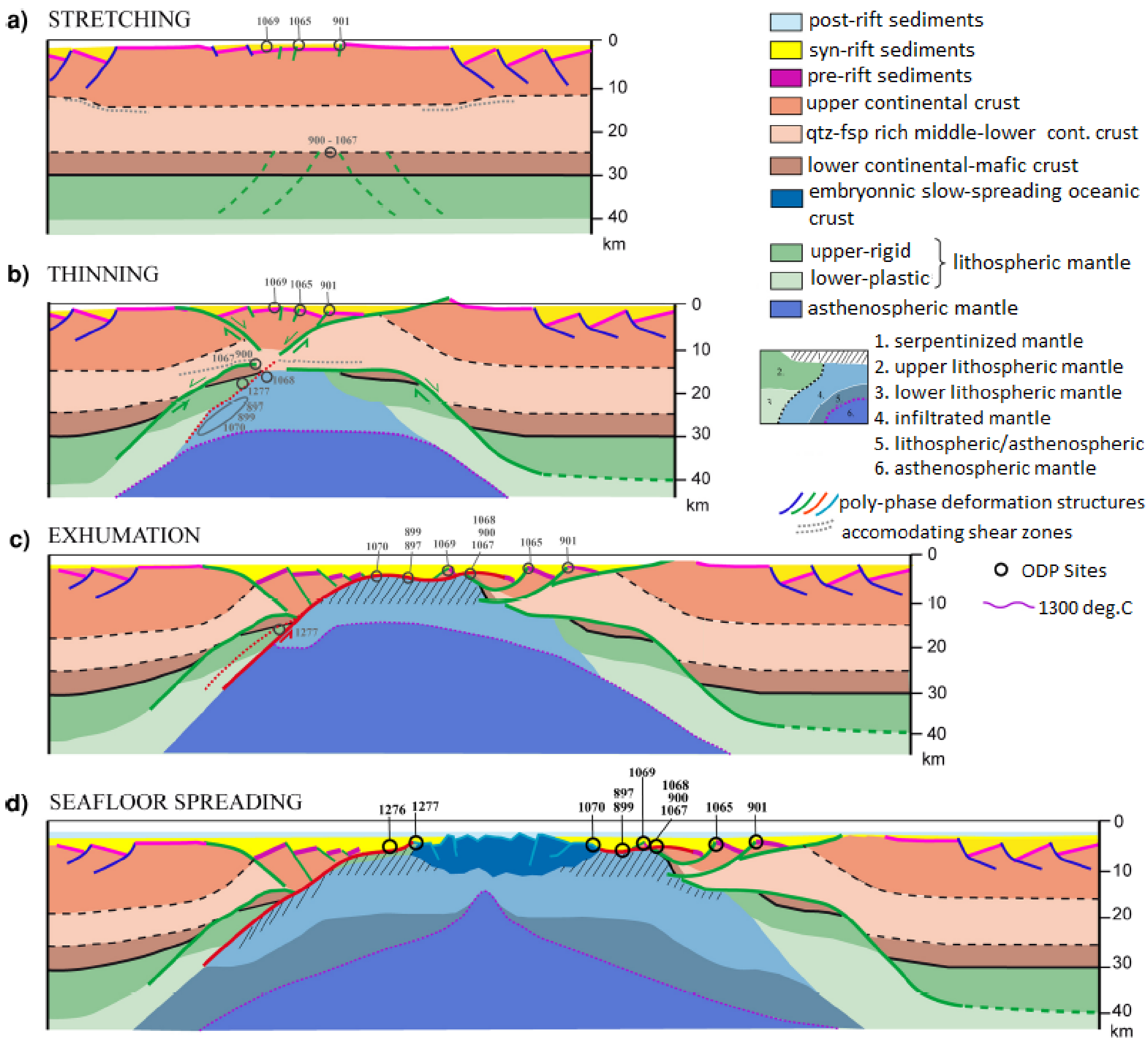

Figure 2.2: Conceptual model showing the evolution of rifting: **a)** The stretching mode is characterized by high-angle listric faulting and half-graben development; **b)** The thinning mode is characterized by a conjugate decoupled system of detachment faults with exhumation of deeper crustal/mantle levels; **c)** The exhumation mode is characterized by detachment faults which crosscut the embrittled crust and exhume serpentinized mantle; **d)** The sea-floor spreading mode is defined by creation of a proto-ridge with localization of thermal and mechanical processes in a narrow zone. The numbers on the top of each figure refer to ODP sites. Modified from Peron-Pindivic and Manatchal [2009].

3 Tectonic setting

In this chapter, the geological evolution and structural setting of the Norwegian Sea Continental Margin will be outlined, with the emphasis on the Vøring and Møre Margins.

Mid-Norwegian margin is a part of the NE Atlantic margin and the North Atlantic igneous province. The margin is located between 62°N and 69°N and divided into two rift segments: the Vøring margin in the north and the Møre margin in the south (Fig.3.1).

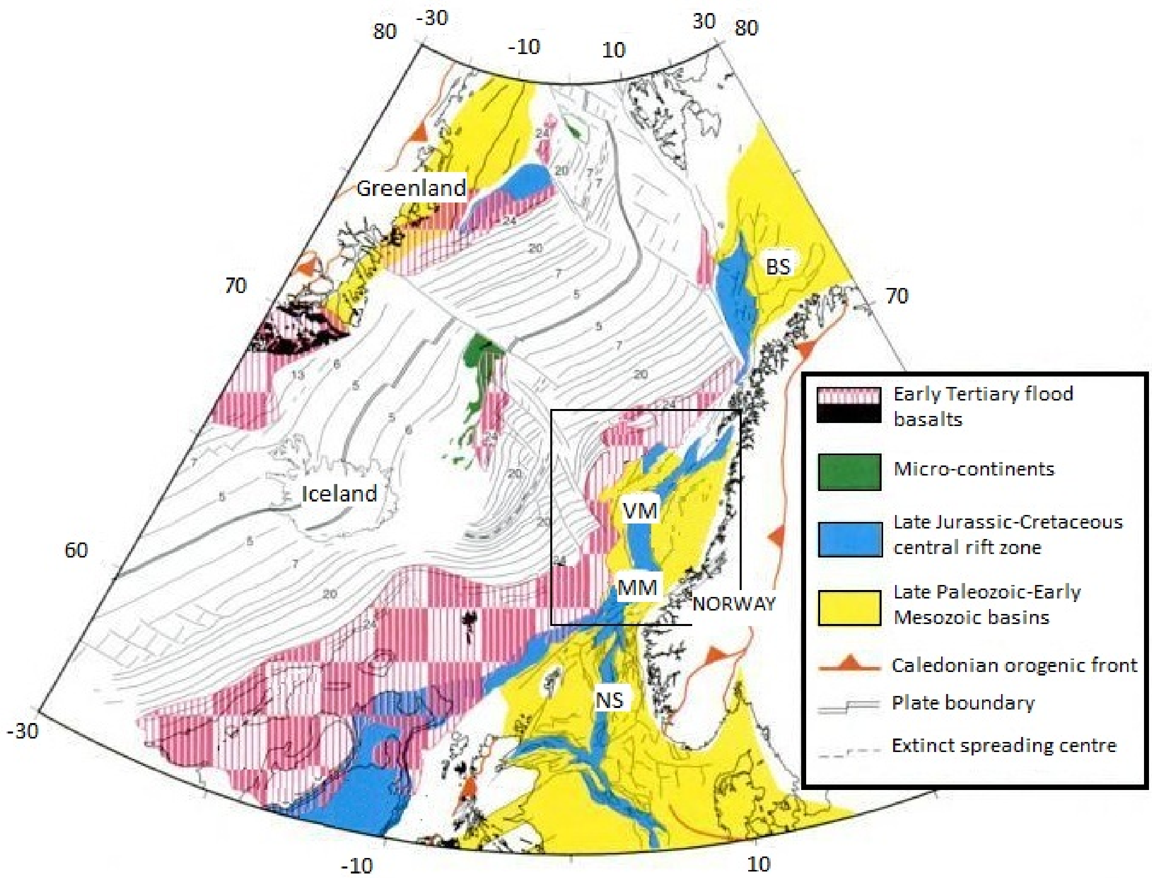

Figure 3.1: Location of the Mid-Norwegian margin with the general structural elements in the NE Atlantic region. The study area with the Vøring and Møre margins is indicated. Magnetic sea-floor spreading anomalies are numbered 3-7, 13, 20, 24. VM, Vøring margin; MM, Møre margin; NS, North Sea; BS, Barents Sea. Modified after Skogseid et al. [2000].

The North Atlantic rift system developed through a series of extensional episodes starting from the Devonian post-orogenic collapse of the Caledonides (≈400 Ma) [Skogseid et al., 2000; Brekke, 2000; Brekke et al., 2001; Zielger, 1988; Lundin and Dore, 1997]. The final rifting episode lasted from the Campanian-Maastrichtian to the break-up in Early Tertiary (≈55 Ma) [Skogseid et al., 2000; Brekke, 2000].

The tectonic history of the North Atlantic margin can in general be divided into the time intervals summarized in Table 3.1. The work in this thesis focuses mainly on the second and third tectonic regimes.

Table 3.1: Three main tectonic periods in the North Atlantic margin tectonic history.

NO.	**Tectonic regimes**	**Main tectonic periods**	**Age(Ma)**
1	Compression	Prior to Devonian (Caledonian orogeny)	>≈400
2	Extension	Late Palaeozoic-Early Cenozoic 1) Late Carboniferous-Permian; 2) Late Jurassic-Cretaceous; 3) Late Cretaceous-Early Tertiary	≈370-≈55
3	Break-up	Early Tertiary (nearly Paleocene-Eocene transition)	≈55

The basins along the NE Atlantic margin share similarities in structures, tectono-magmatic style and timing (Fig.3.2) [Lundin and Dore, 1997]. Therefore it is favorable to show the margin as a whole in the regional NE Atlantic settings, following by closer insight into the study area and structural settings of the Vøring and Møre basins.

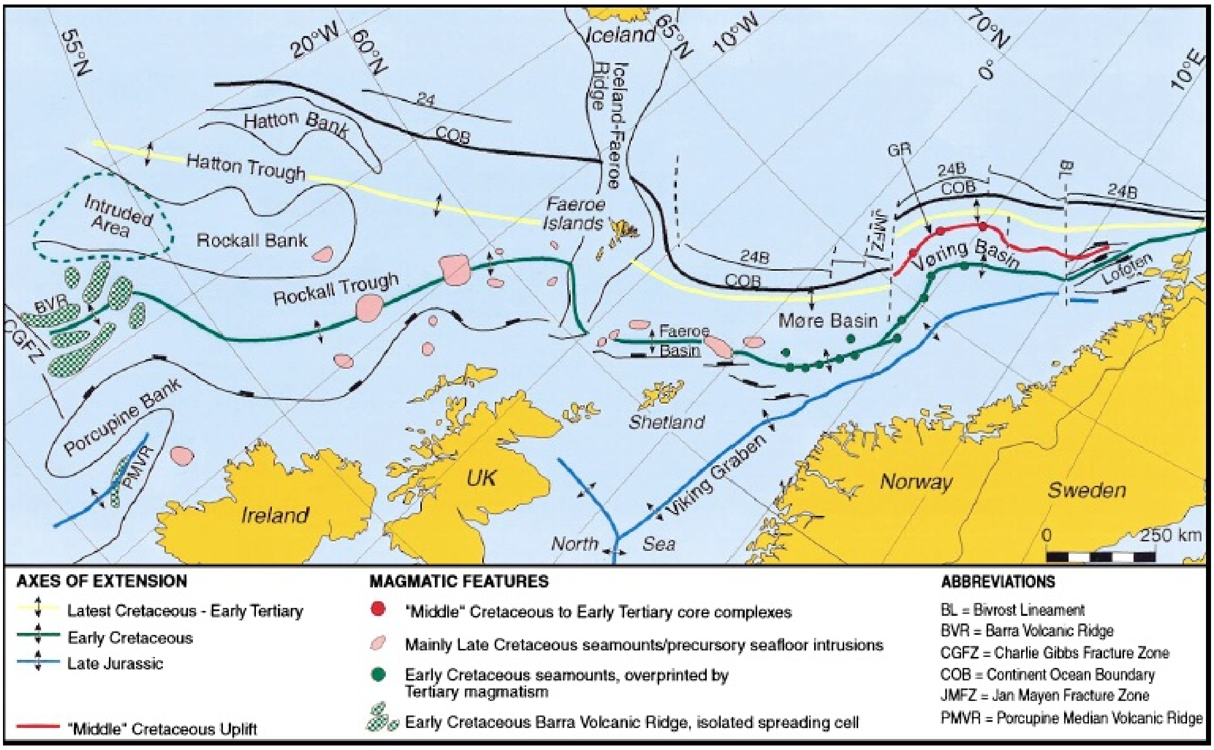

Figure 3.2: Simplified map of the NE Atlantic margin. The map showing migration of the rift system northwards from Late Jurassic to Early Tertiary along the NE Atlantic margin [Lundin and Dore, 1997].

3.1 Regional NE Atlantic setting

Although more detailed maps are now available locally, we use the Brekke et al. [2001] and Brekke [2000] maps in order to illustrate the regional large scale evolution of the overall NE Atlantic.

The geologic time scale used in this thesis is edited by Gradstein et al. [2004].

3.1.1 The Caledonian orogeny

Four orogenic events within the Caledonian orogen are recognized in Norway: Finnmarkian (Late Cambrian), Trondheim (Early Arenig), Taconian (Mid-Late Ordovician) and Scandian (Mid Silurian-Early Devonian) [Roberts, 2003]. The first two events involved accretion between Baltica and/or adjacent microcontinent and Iapetan arcs. The Mid-Late Ordovician event is the arc accretion event within the Laurentian margin. During Silurian-Devonian times, the Iapetus Ocean underwent closure and the Baltoscandian margin of Baltica was subducted beneath Laurentia. The development of the Caledonian mountain belt was marked by series of eastward allochthons thrust onto Archaean and Proterozoic crystalline rocks of the Fennoscandian Shield, and development of the foreland basins onshore Norway [Zielger, 1988; Roberts, 2003].

3.1.2 Late Carboniferous - Permian extensional setting

Carboniferous and Permian times represent the period of active tectonics along the NE Atlantic margin. In the Middle to Late Devonian the Caledonides collapsed changing the tectonic evolution from compression to extension. The change into divergent settings caused the development of major basement shear zones and half-graben basins, as e.g. the Hornelen Basin onshore Norway, filled with thick successions of intra-continental deposits [Zielger, 1988; Andersen and Jamtveit, 1990; Andersen et al., 1994; Hartz and Andresen, 1997].

Zielger [1988] interpreted the main Late Palaeozoic rift episodes to have taken place in Mid-Carboniferous, Carboniferous-Permian and Permian-Early-Triassic times. Fig.3.3 shows the paleogeography of Early Carboniferous times plotted on a 300 Ma plate reconstruction. The rift system was dominated by N-S to NE-SW-trending normal faults with NW-SE-trending transfer faults. The rifting system is filled mainly with continental clastics [Brekke et al., 2001].

The Permian times were a time of major plate reconfiguration, expressed as an extension which marked the onset of the break-up of the Pangean supercontinent.

The marine transgressive/regressive phases change is a characteristic feature of the Triassic period. The period of thermal relaxation has been reported from the Middle Triassic to Early Jurassic times. Brekke et al. [2001] reported block-faulted terrain formation from that time. On the continental margin off central Norway, the tectonic activity was concentrated on the Trøndelag Platform and Halten Terrace (described further in this chapter), and affected large parts of the area with NNE-SSW normal faults.

3.1.3 Late Jurassic - Cretaceous extensional setting

Lundin and Dore [1997] proposed that by Late Jurassic - Early Cretaceous, rifting of the NE Atlantic propagated northeastward through the Rockall Trough, West Shet-

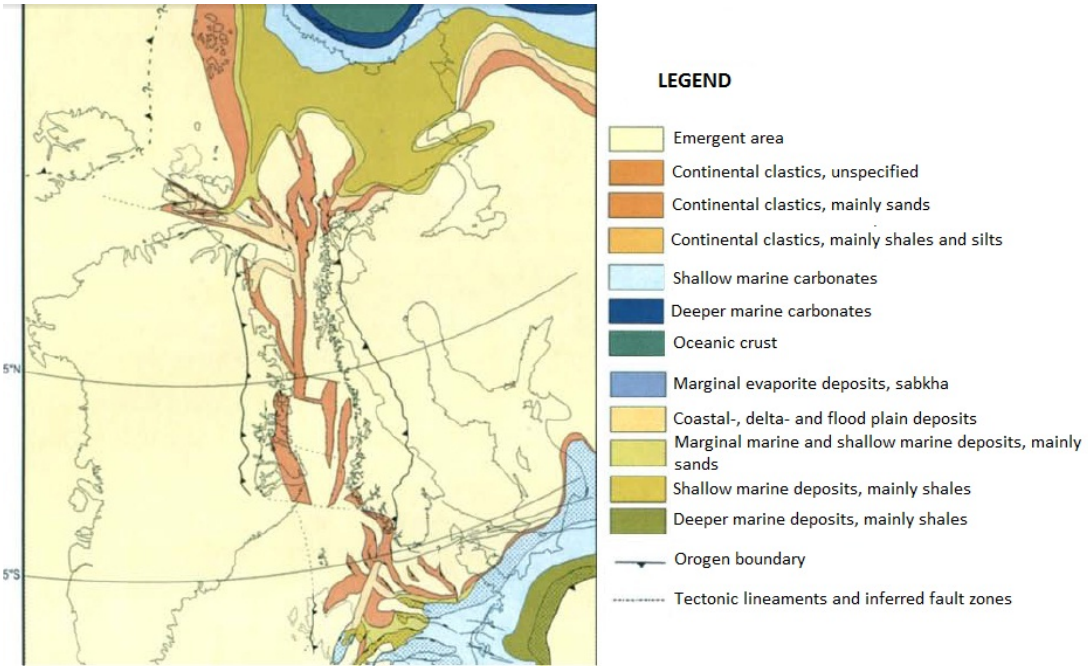

Figure 3.3: The paleogeography of Early Carboniferous times plotted on a 300 Ma plate reconstruction. The rifting system is filled mainly with continental clastics at that time [Brekke et al., 2001].

land/Faeroe Trough, central Møre Basin and eastern Vøring Basin (Fig.3.2) contemporaneously with rifting in the Labrador Sea.

Combination of the fluctuation in sea level and tectonic variations with uplift and rapid subsidence caused favorable conditions for the accumulation of black shales, which have a good source rock potential [Brekke et al., 2001; Zielger, 1988].

Fig.3.4 shows the paleogeography of Early Cretaceous times plotted on a 70 Ma plate reconstruction map.

3.1.4 Late Cretaceous - Early Tertiary extensional setting

Late Cretaceous is characterized by an intriguing and debated tectonic episode in the Norwegian - Greeenland Sea. The global sea level reached its maximum in the Late Cretaceous, when the area between Norway and Greenland was an epicontinental sea in which crust had been attenuated by the multiple post-Caledonian rift events. The tectonism was expressed as faulting, accelerated basin subsidence and conjugate uplift, tilting of the bounding platforms areas to the major basins, as e.g. Møre and Vøring Basins. The flanks of the basins were deeply eroded. The onset of Late Cretaceous tectonic episode and accelerated subsidence of the Vøring and Møre basins coincides with the rapid subsiding of basins along the Barents Sea margin.

The final Maasctrichtian - Paleocene rifting event have possibly started in the Late Maastrichian time [Lundin and Dore, 1997]. There is a little tectono-stratigraphic evidence of timing of the onset of Late Cretaceous - Paleocene episode leading to complete lithospheric break-up. However, Skogseid et al. [2000] assumed that this episode lasted for c. 20 Ma leading into the onset of sea-floor spreading at the Paleocene - Eocene transition. The event was associated with the regional uplift of the Norwegian - Greenland rift system possibly due to increased heat flow just prior to break-up.

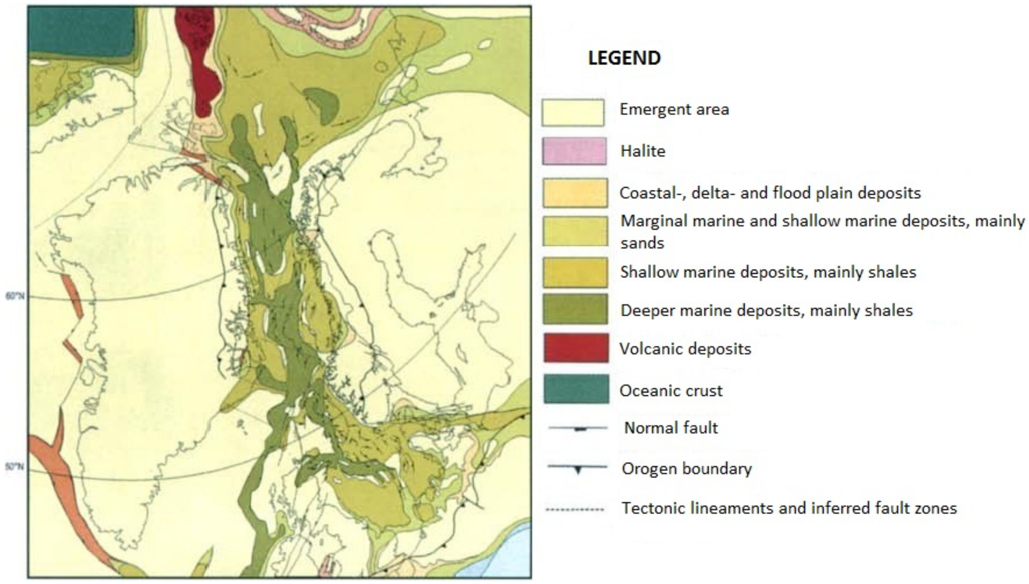

Figure 3.4: The paleogeography of Early Cretaceous times plotted on a 70 Ma plate reconstruction. The rifting system is filled with shallow and deeper marine deposits, mainly shales [Brekke et al., 2001].

3.1.5 Early Tertiary break-up setting

The final Maastrichtian-Paleocene rift episode led to the separation and onset of seafloor spreading in the Paleocene-Eocene transition [Lundin and Dore, 1997; Skogseid et al., 2000] (Fig.3.5). This event led to the 300 km wide zone with lithospheric thinning and post-break subsidence. The resulting break-up between Eurasia and Greenland was accompanied by extensive volcanism.

The North East Atlantic Ocean is furthermore characterized by the presence of numerous and voluminous magmatic material, encompassing flood basalts, mafic and ultramafic complexes. This corresponds to the so-called North Atlantic Igneous Province (NAIP). The formation and origin of the NAIP has been discussed and challenged over the past ten years, and still remains under debate. Meyer et al. [2007] has tested the most prominent geodynamic models (e.g. delamination, impact, fertile mantle, small-scale convection, and mantle plume) in order to constrain the possible origin of the anomalous volumes of magma in the region. The authors came to the conclusion that the mantle plume concept is the most successful in explaining the formation of the NAIP. However, the authors also noted that this is largely due to 'the adaptations that have been made to the site-specific model over the years to better explain observations of the province'. The other models (rift-related small-scale convection) also appear to explain magma-rich margins but need to be 'further matured' to correctly explain the overall geologic context of the area (e.g. the Iceland-Faroe Ridge for example).

3.1.6 From rift to drift

During plate separation in Early Eocene time, an intriguing unconstrained compressive regime gave raise to inversion structures along the North-East Atlantic margins [Lundin and Dore, 1997]. The Norwegian-Greenland Sea margins have been subject to post breakup deformation, mainly compressional, but also extensional [Lundin and Dore, 2002].

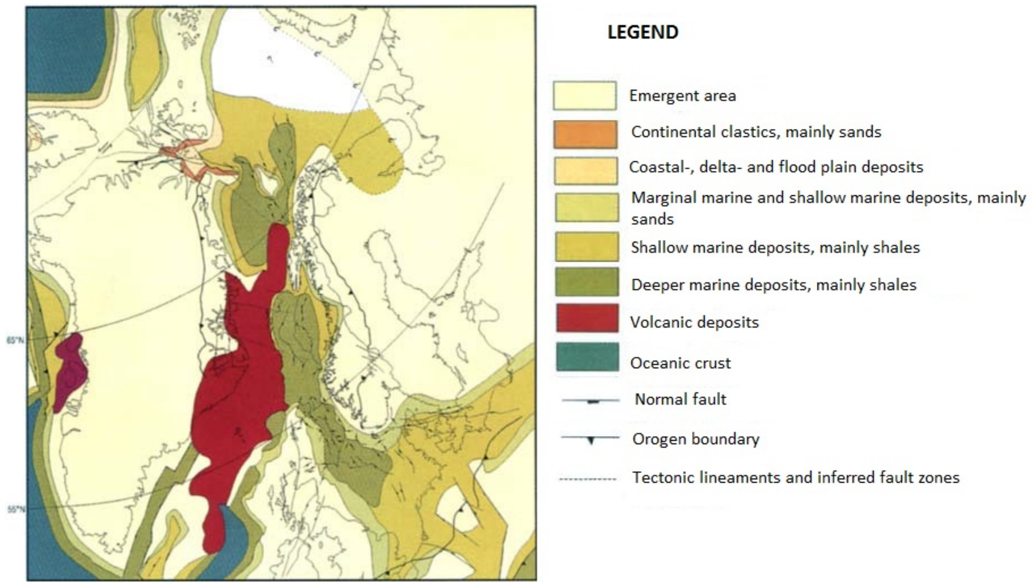

Figure 3.5: The paleogeography of Early Eocene times plotted on a 53 Ma plate reconstruction. The sedimentary environment of the Tertiary at the Palaeogene transition from rift to drift settings [Brekke et al., 2001].

Compressional deformation in the mid-Norwegian margin is shown by local domes with reverse-movement of normal faults (e.g. Helland-Hansen Arch) [Blystad et al., 1995; Brekke, 2000].

Plate reorganization of Oligocene-Miocene age led to the renewed extension of the North-East Atlantic margins [Lundin and Dore, 2002].

The last major tectonic event on the NE Atlantic margins was regional uplift of Neogene age. Lundin and Dore [2002] report that the size and magnitude of this uplift is much larger than that of the mid-Cenozoic domes. This uplift caused an increase in sediment supply and westward progradation of the deltaic systems. A major sedimentary wedge of Pliocene age progrades away from the mainland with consistent pattern around most of the Norwegian mainland.

The Pleistocene period is known as a period of repeated glaciations. Repeated advances and retreats of Scandinavian ice sheet led to erosion and deposition of an ice-related sediments. The uplift occurred in several phases during Cenozoic, and the main component of uplift took place in Late Pliocene and Pleistocene time and was associated with glaciations [Lundin and Dore, 2002].

3.2 Continental margin off central Norway

The Vøring and Møre Basins were formed as a result of the Late Jurassic-Early Cretaceous rifting episode and they both have a thick Cretaceous sedimentary infill (Fig.3.6 and 3.7, for location of the seismic transects see Fig.3.8). The deep Cretaceous basins have up to 13 km of sediments, of which 8-9 km comprise the Cretaceous succession [Blystad et al., 1995; Osmundsen et al., 2002; Brekke et al., 2001; Brekke, 2000; Skogseid et al., 2000].

The Geoseismic sections from Brekke [2000] and Osmundsen et al. [2002], presented in Fig.3.6 and 3.7, are used further as a first-order constraint to build a crustal structure of the margin (Chapter 6).

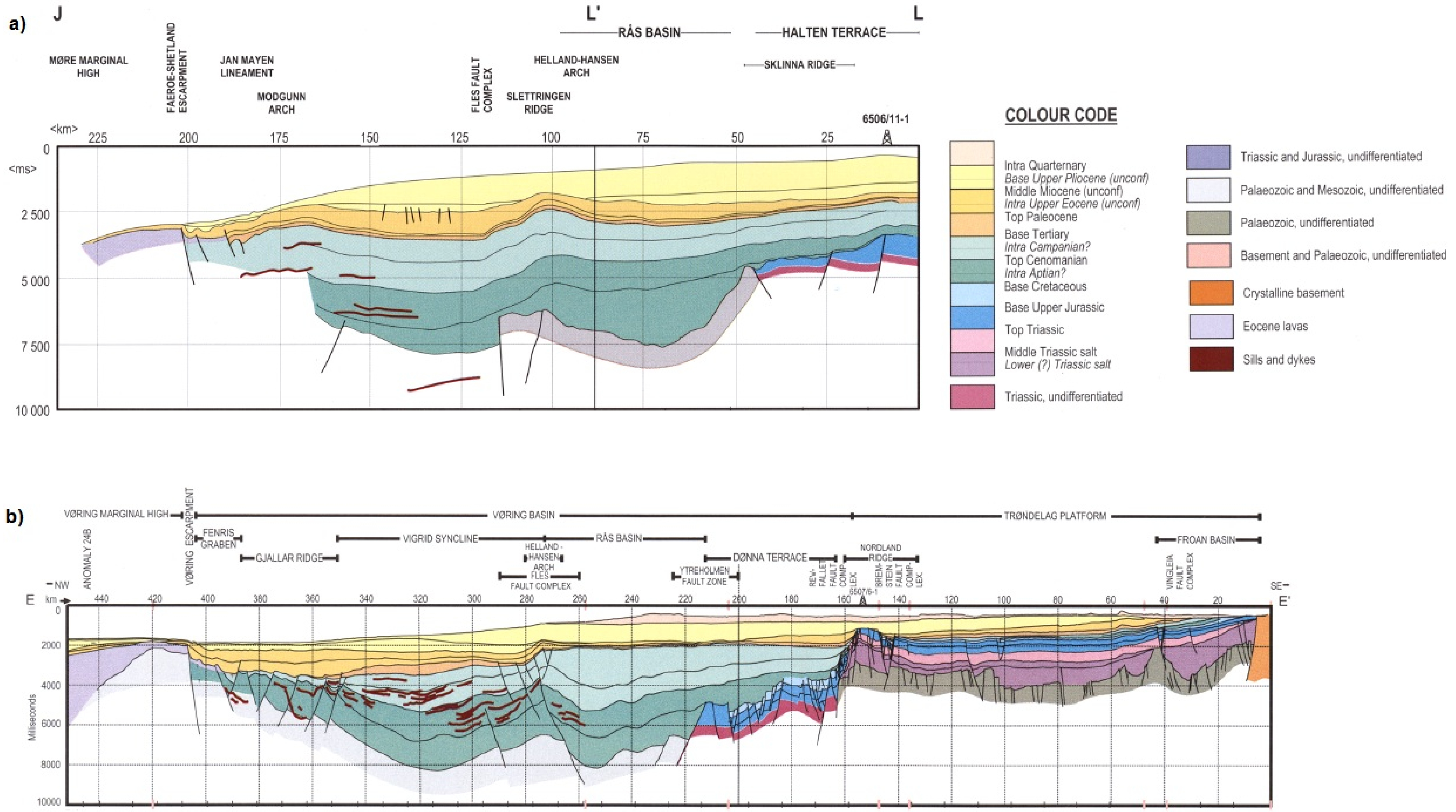

Figure 3.6: Geoseismic sections from Brekke [2000]: **a)** section JL'L and **b)** section EE'. See Fig.3.8 for the line locations.

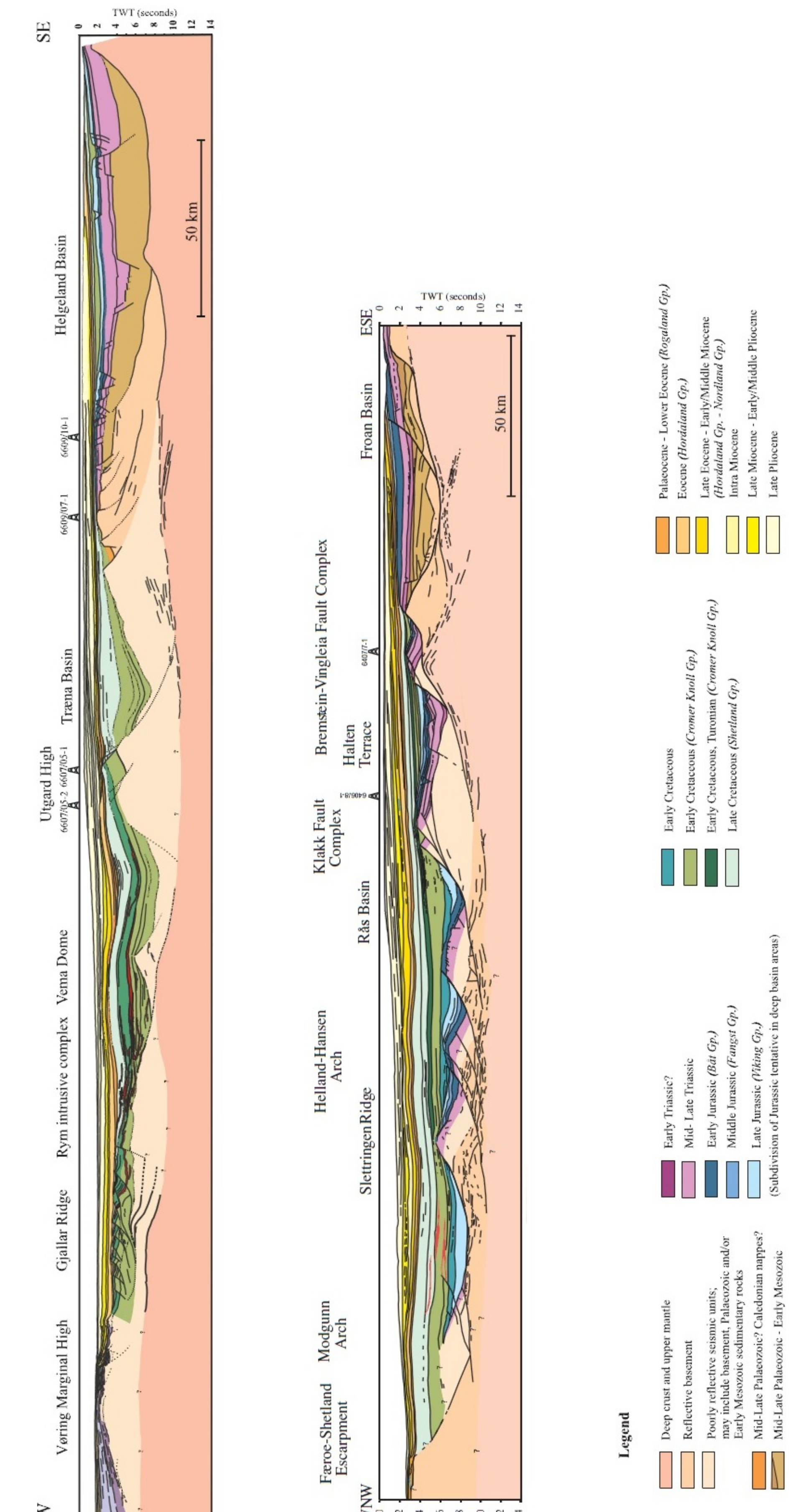

Figure 3.7: Geoseismic sections from Osmundsen et al. [2002]: **a)** section 7 and **b)** section 6. See Fig.3.8 for the line locations.

Skogseid et al. [2000] reported that the Møre and Vøring Basins formed primarily as a result of the Late Jurassic-Early Cretaceous rifting. However, Early Cretaceous faulting is difficult to constrain due to poor seismic resolution below the thick Cretaceous sedimentary strata. Fault activity along the edge of the Trøndelag Platform and at the Halten and Dønna Terraces has been reported by Blystad et al. [1995] and Brekke [2000] in Early Cretaceous time. Osmundsen et al. [2002] made an observation that Palaeozoic-Early Mesozoic structures had been reactivated during the phase of Mesozoic rifting in the Trøndelag Platform area. The age of faulting under the east-central parts of the southern Vøring/northernmost Møre Basin is suggested by Osmundsen et al. [2002] to be Jurassic to earliest Cretaceous in age.

The axis of the Early Cretaceous rift as located in the western parts of the Vøring Basin [Osmundsen et al., 2002; Lundin and Dore, 1997] (Fig.3.2). The axial areas experienced doming and uplifts all the way from the south of Ireland to the borders of the Barents Sea [Lundin and Dore, 1997]. This regional uplift could be linked to the onset of crustal extension and increased heat flow. The basins were subject to the highest elevation (thermal domes) and deepest erosion (erosional unconformity) in the Middle Jurassic/earliest Cretaceous rifting phase, what implies that Jurassic deposits might be missing in the deep Møre and Vøring Basins [Brekke, 2000; Brekke et al., 2001]. Osmundsen et al. [2002] suggested that the location of the rift axis was controlled by a low-angle normal fault with displacement in the order of tens of kilometers, that might bring Jurassic and Early Cretaceous strata into contact with strongly reflective lower crust. In the most highly attenuated area of the basin, the sedimentary rocks might rest directly upon the strongly reflective lower crust, across a flat-lying reflector interpreted by Osmundsen et al. [2002] as a low-angle detachment fault with horizontal separation of 25-35 km. This result is coherent with refraction measurements that show that only 2-3km crustal rocks remain in the central part of the deep basin [Raum et al., 2002].

3.2.1 Main structural settings

The two rift segments, the Vøring margin in the north and the Møre margin in the south (see Fig.3.1 for the location), have some similar structural characteristics, such as marginal highs, escarpments and deep Cretaceous basins (Fig.3.8).

The basins to the west are flanked by the Møre and Vøring Marginal Highs. The boundary between the marginal highs and the basin area is marked by the Faeroe-Shetland Escarpment to the south and the Vøring Escarpment to the north. The Møre Basin is flanked to the east by the uplifted mainland, and the Vøring Basin - by the Trøndelag Platform.

To the north, the deep Vøring Basin area is bounded by the NW-SE trending Bivrost Lineament, separating the basin from the narrow Lofoten ridge. The Jan Mayen lineament separates the Vøring Basin to the north and the Møre Basin to the south. These two lineaments continue oceanwards respectively as the Bivrost and the Jan Mayen fracture zones. They possibly reflect an old structure in the crystalline basement [Brekke, 2000]. The lineaments could have controlled the post Caledonian development of the continental margin off central Norway, as they divide the margin into segments and could act as controlling transfer zones in a crustal extension zone between Norway and Greenland [Brekke, 2000].

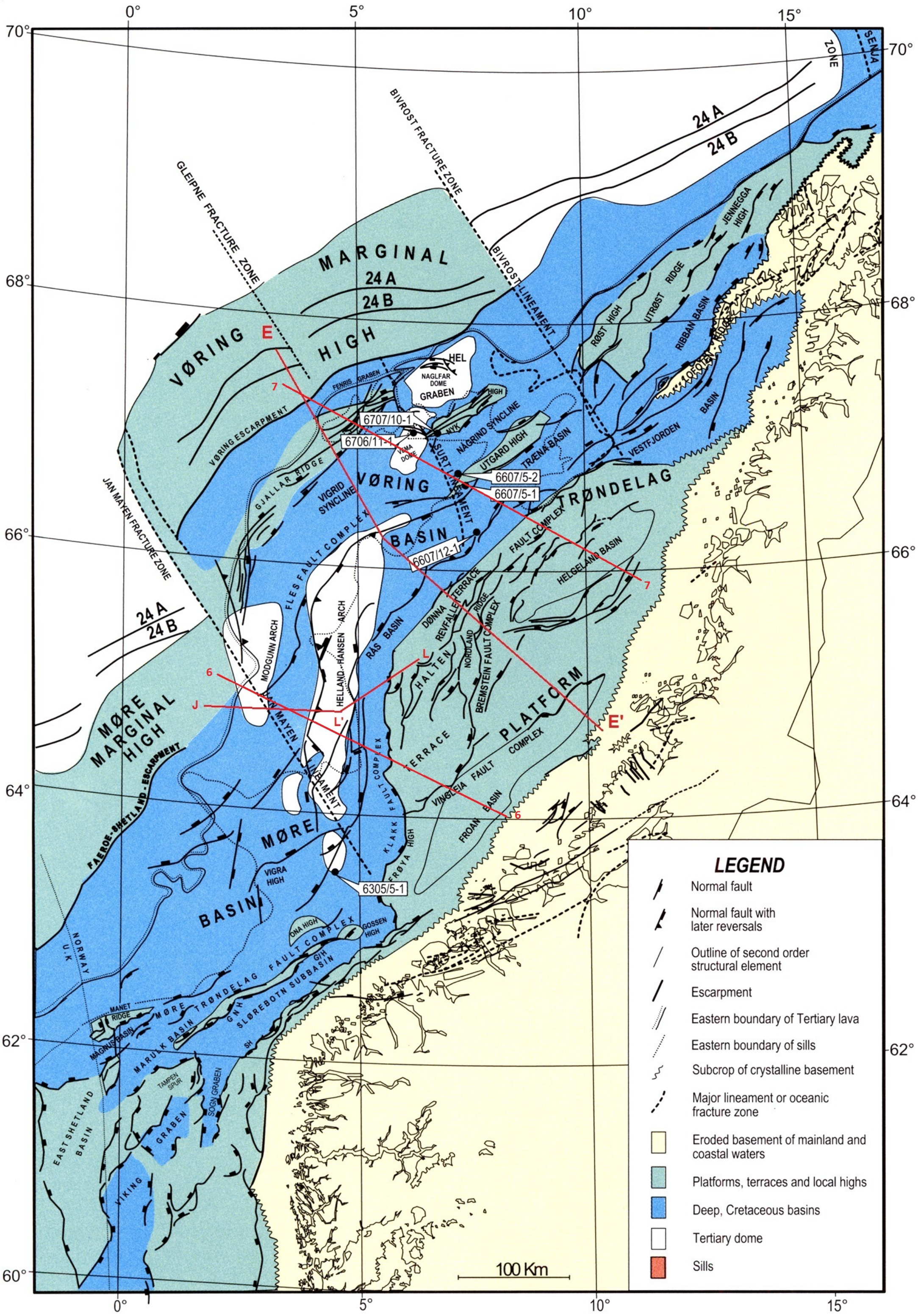

Figure 3.8: Structural map of the Norwegian Sea continental margin from Brekke [2000], here with the Geoseismic transects shown in Fig.3.6 and 3.7.

The detailed structural and tectonic settings of the continental margin off central Norway are found in the thorough reviews of Brekke [2000] and Osmundsen et al. [2002].

3.2.2 The Vøring margin

The overall framework of the Vøring Margin shows the NE-SW trending deep Cretaceous Basin, flanked by highs, platforms and elevated mainland. The Vøring Basin together with the Vøring Marginal High and the Trøndelag Platform forms the so-called Vøring continental margin (Fig.3.8).

The Vøring Basin has experienced several extensional and compressional episodes that led to the diversity of structures such as grabens, sub-basins and structural highs. One of the main tectonic episodes took place in the Carboniferous to Late Permian and produced horsts and half-grabens on the **Trøndelag Platform** . The major faults were tectonically active through Triassic time, giving rise to NE-trending basins, filled with Triassic and Upper Palaeozoic sediments (e.g. the Froan basin in the south). The Trøndelag Platform has been mostly stable since the Jurassic and is covered by flat-laying strata. The subdivision into the deep basins to the west and the platform area to the east was possibly initiated in the early stage of the late Mid-Jurassic to Early Cretaceous tectonic episode [Brekke, 2000]. The evidence of the terrace-basin boundary faulting had been reported by Osmundsen et al. [2002]. The southern Vøring Basin is bounded by large-magnitude, moderate- to low-angle normal faults that are well-imaged on the long-offset seimic data with variations in geometry and amount of displacement. The Dønna and Halten Terraces were initiated by faulting in Late Jurassic time with the main subsidence in Cretaceous time [Brekke, 2000] (Fig.3.8). The southern Trøndelag Platform-Halten Terrace boundary is constituted by the Bremstein-Vingleia Fault Complex (BVFC) [Brekke, 2000; Blystad et al., 1995]. A well defined fault-plane reflection reveals the ramp-flat geometry of the BVFC in the seismic data [Osmundsen et al., 2002] (Fig.3.7). The sediment thickness of the Trøndelag Platform is very different from the Vøring Basin: the Cretaceous strata are thin and partly absent here, which could be explained by uplift and deep erosion in the Late Cretaceous [Brekke, 2000] (Fig.3.6 and 3.7). Sedimentation patterns on the Halten and Dønna Terraces are characterized by wedge-shaped reflection packages of Late Triassic to Late Jurassic age which are banked against the Revfallet and BVFC Complexes [Osmundsen et al., 2002] (Fig.3.7).

The **Vøring Basin** area is furthermore bisected by the Fles Fault Complex which runs from the Jan Mayen Lineament in the south to the Bivrost Lineament in the north. The complex probably originated in the Mid-Late Jurassic as normal faults and experienced several phases of reactivations. The other tectonic boundary in the basin is the Surt Lineament which runs parallel to the other two lineaments and is obviously controlled by the same tectonic settings. The Surt Lineament acted as a depocenter before the formation of the synclines and highs in the Late Cretaceous. The Gjallar Ridge in the western part of the basin was initiated in the Late Cenomanian-Early Turonian time [Brekke, 2000; Gernigon et al., 2004]. Gernigon et al. [2003, 2004] studied the deep structures underlying the north Gjallar Ridge (named the T-reflection) and the subsurface deformation. Faulted structures located on the top of crustal dome (Fig.3.7) are proved to be Early Campanian-Maastrichtian synrift formations. The relative uplift and faulting above the T-reflection is explained as a 'boudinage' and differential compaction of the sedimentary section, which was controlled and accommodated in depth by the pre-existing dome, developed during the rifting stage. The authors proposed that the crustal dome influenced the structural development of the sedimentary basin just prior the breakup stage. The whole basin was uplifted at the beginning of Tertiary period due to the regional uplift of the Norwegian - Greenland rift system. The uplift might be a response to heat flow just prior to break-up [Skogseid et al., 2000]. The uplift event is recorded as a hiatus on the Vøring and Møre Basins flanks, also across highs and domes within the Vøring Basin (e.g. Gjallar Ridge) [Brekke, 2000; Gernigon et al., 2004]. Sediments were deposited in shallow synclinal areas within the basin, while in the Møre Basin, thick Paleocene/early Eocene sedimentary successions are documented as prograding into the basin from platforms [Brekke et al., 2001; Brekke, 2000; Lundin and Dore, 1997]. The Helland-Hansen Arch in the southern part of the basin is believed to be formed between Middle Eocene and End Oligocene time due to compressional deformation of the margin [Lundin and Dore, 2002]. This phase followed the Paleocene-Eocene igneous activity.

The Vøring Marginal High comprises Tertiary sediments on top of thick Lower Eocene flood basalts. The high is bounded to the west by oceanic crust [Brekke, 2000]. Early Cretaceous basin formation is believed to be a result of thermal subsidence after the main rifting episode in Jurassic-Early Cretaceous time [Brekke, 2000].

3.2.3 The Møre margin

The Møre Basin is bounded to the north by the Jan Mayen Lineament, to the south-east by the Møre-Trøndelag Fault Complex and to the west by the Faeroe-Shetland Escarpment (Fig.3.6, 3.7 and 3.8).

In contrast to the Vøring Basin, it has been proposed [Brekke, 2000] that the **Møre Basin** has been tectonically quiet after the Mid-Jurassic - Early Cretaceous rifting. However, alternative scenarios are also proposed in which the formation of the deep sag basins correspond to periods of high tectonic activity [Peron-Pindivic et al., 2012a,b]. The basin experienced passive subsidence with no tectonic activity in the Late Cretaceous, and only minor activity in Tertiary time [Brekke, 2000].

The **Møre-Trøndelag Fault Complex** represents a system of fault controlled ridges, highs and minor basins which were originated as a system of horsts and half-grabens in Triassic times, but were reactivated in several episodes during the following tectonic history [Brekke, 2000; Blystad et al., 1995].

Like the Vøring Marginal High, the **Møre Marginal High** includes Tertiary sediments on the top of thick early Eocene flood basalts. Brekke [2000] reports the westward thinning of the Cretaceous units in the basin which indicates that Cretaceous units are very thin or missing beneath the lavas on the high. Brekke [2000] also reports the early lavas flowed eastward of the present escarpment, which might be caused by normal faulting in the high, which separated ”inner flows” from the marginal high.

The position of the ocean-continent transition (OCT), as well as nature of the underlying basalt flows substrate in the continental part of the highs, has not been clearly resolved in the geophysical data and is still a matter of debate.

4 Dataset

In order to obtain a better geological understanding of the study area, combined interpretation of seismic, gravity and magnetic data has been undertaken.

4.1 Potential Field Data

The gravity and magnetic data used for the modeling are a compilation from the Geological Survey of Norway (NGU).

The magnetic grid used in this study consists of a compilation of all pre-existing ship track and aeromagnetic data available. It has been published by Olesen et al. [2010a]. The original surveys have been reprocessed using modern levelling techniques [Mauring and Kihle, 2006] and merged with two new high-resolution aeromagnetic datasets. Systematic adjustments were applied using the minimum curvature suturing function of the Gridknit software Geosoft (2005).

The gravity data used in this study is also from the regional compilation of Olesen et al. [2010a,b]. This compilation is based offshore on approximately 59 000 km of various shipboard gravity measurements provided by the Norwegian Petroleum Directorate, oil companies, and the Norwegian Mapping Authority. The data were merged with previous Geosat and ERS-1 satellite compilations available in the deep-water areas of the Norwegian-Greenland Sea [Andersen et al., 2008; Laxon and McAdoo, 1994]. The surveys have been levelled using the International Standardization Net 1971 (IGSN 71) and the Gravity Formula 1980 for normal gravity. The combined dataset has been interpolated to square cells of 1 km size using the minimum curvature method. A density of 2400 kg/m3 was used to calculate the complete Bouguer correction of the free air anomaly along the survey area.

Bathymetric data used for Bouguer correction in the deep-water part of the map is based on the satellite altimetry data of Sandwell and Smith [1997].

Fig.4.1 - 4.4 show structural and bathymetry maps, as well as gravity and magnetic anomaly maps of the study area. The bathymetry, gravity- and magnetic anomaly maps are generated with a help of the Geosoft software using the UTM (Universal Transverse Mercantor) projection with the 32UTM zone. All maps show the location of the two seismic transects used for the seismic interpretation (see next section).

4.2 Seismic Data

The seismic data used in this thesis includes reflection and refraction data. Two seismic reflection profiles have been studied in details: the VBT9401 and VMT95007 which are in the public domain and available through the DISKOS database. The VBT9401 profile (Geoseismic Transect AA' here) is from a 2D survey of the Vøring Basin shot by Geoteam for NOPEC, recorded to 12000 ms. The VMT95007 (Geoseismic Transect BB' here) is from a 2D survey of Møre and Vøring basins shot by PGS for NOPEC, recorded to 12000

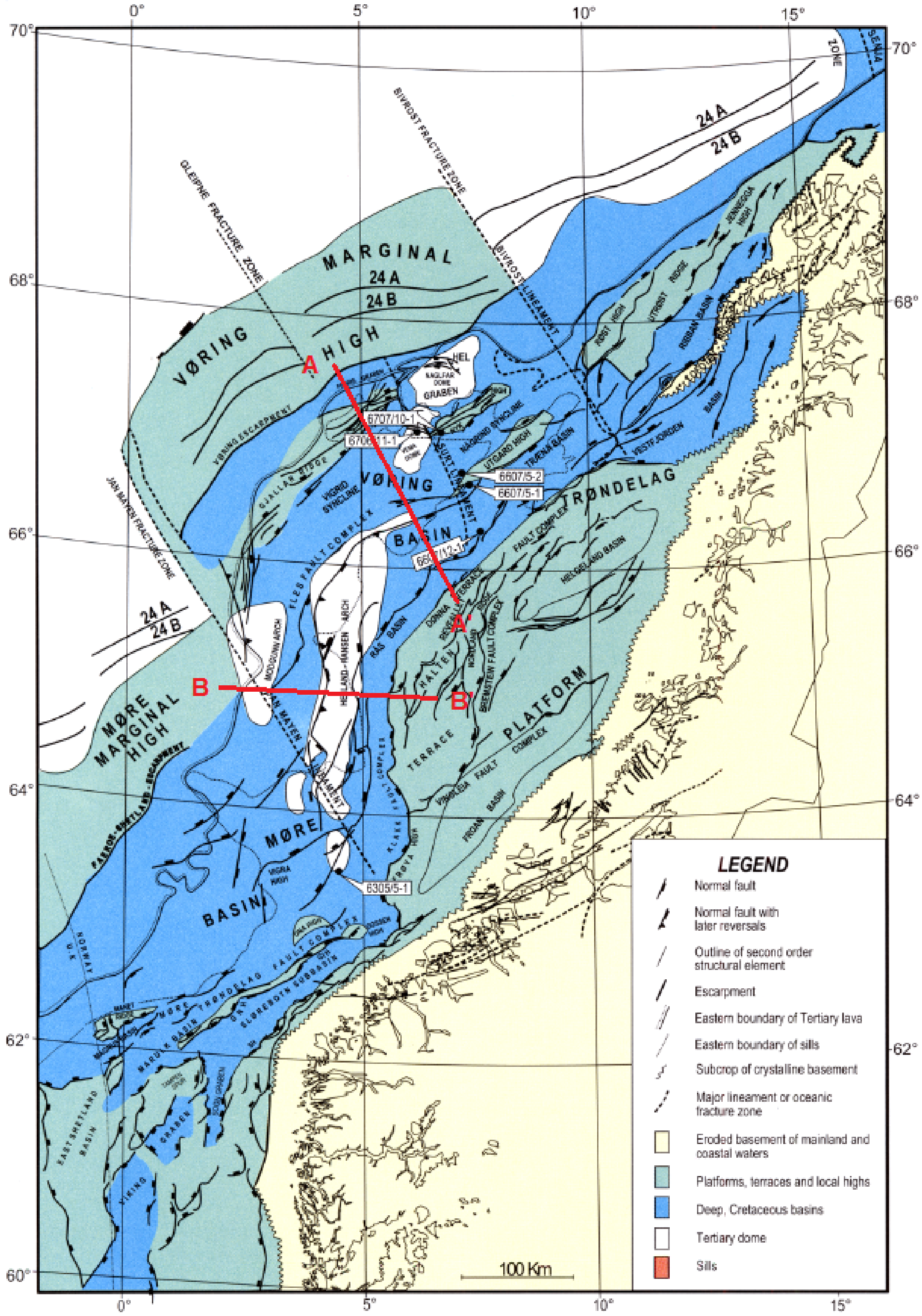

Figure 4.1: Structural map of the study area, here with the Geoseismic transects AA' and BB' used for the seismic interpretation. The transects are shown in Fig.4.5. Modified from Brekke [2000].

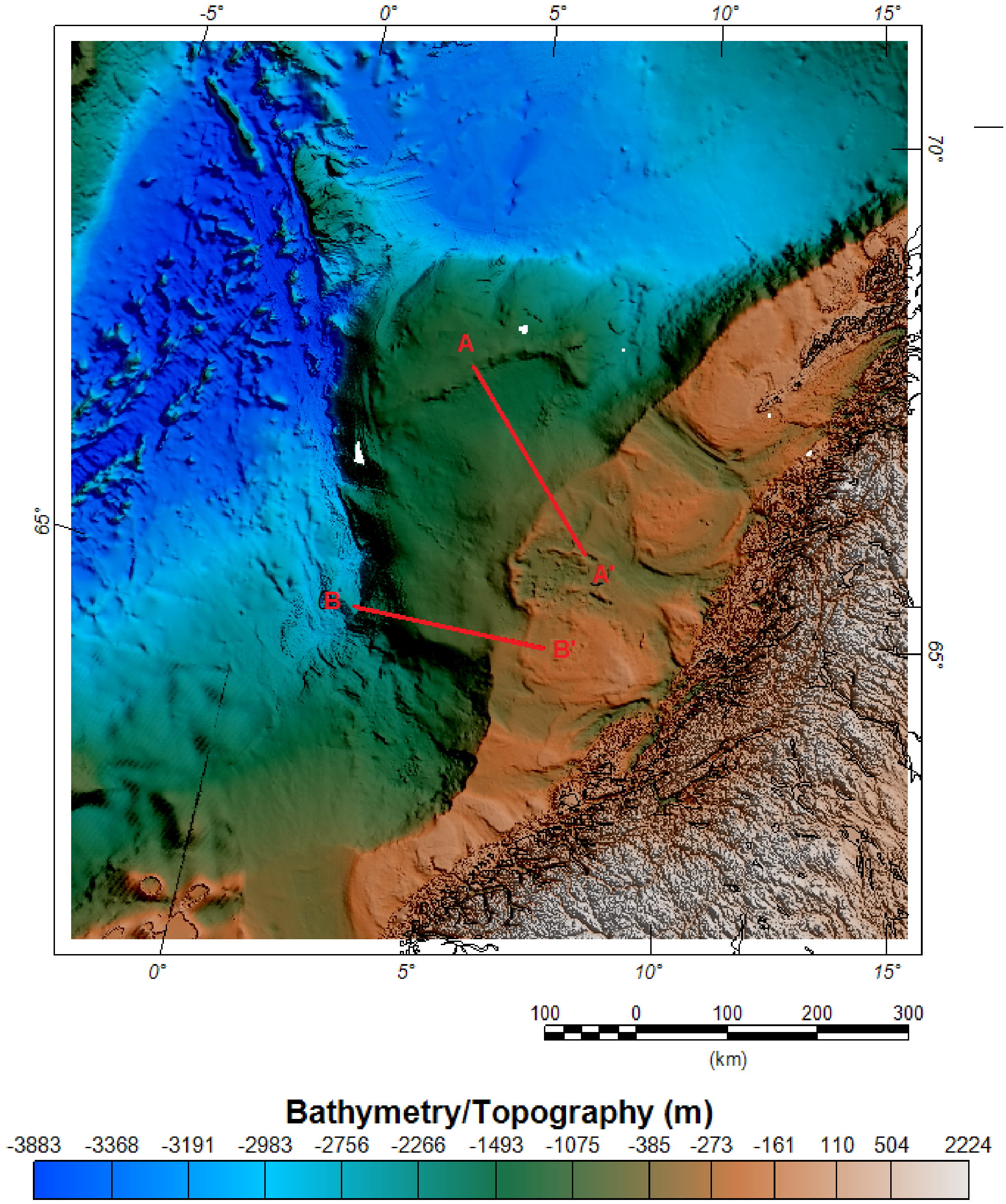

Figure 4.2: Bathymetry/Topography map of the study area, here with the Geoseismic transects AA' and BB' used for the seismic interpretation. The transects are shown in Fig.4.5.

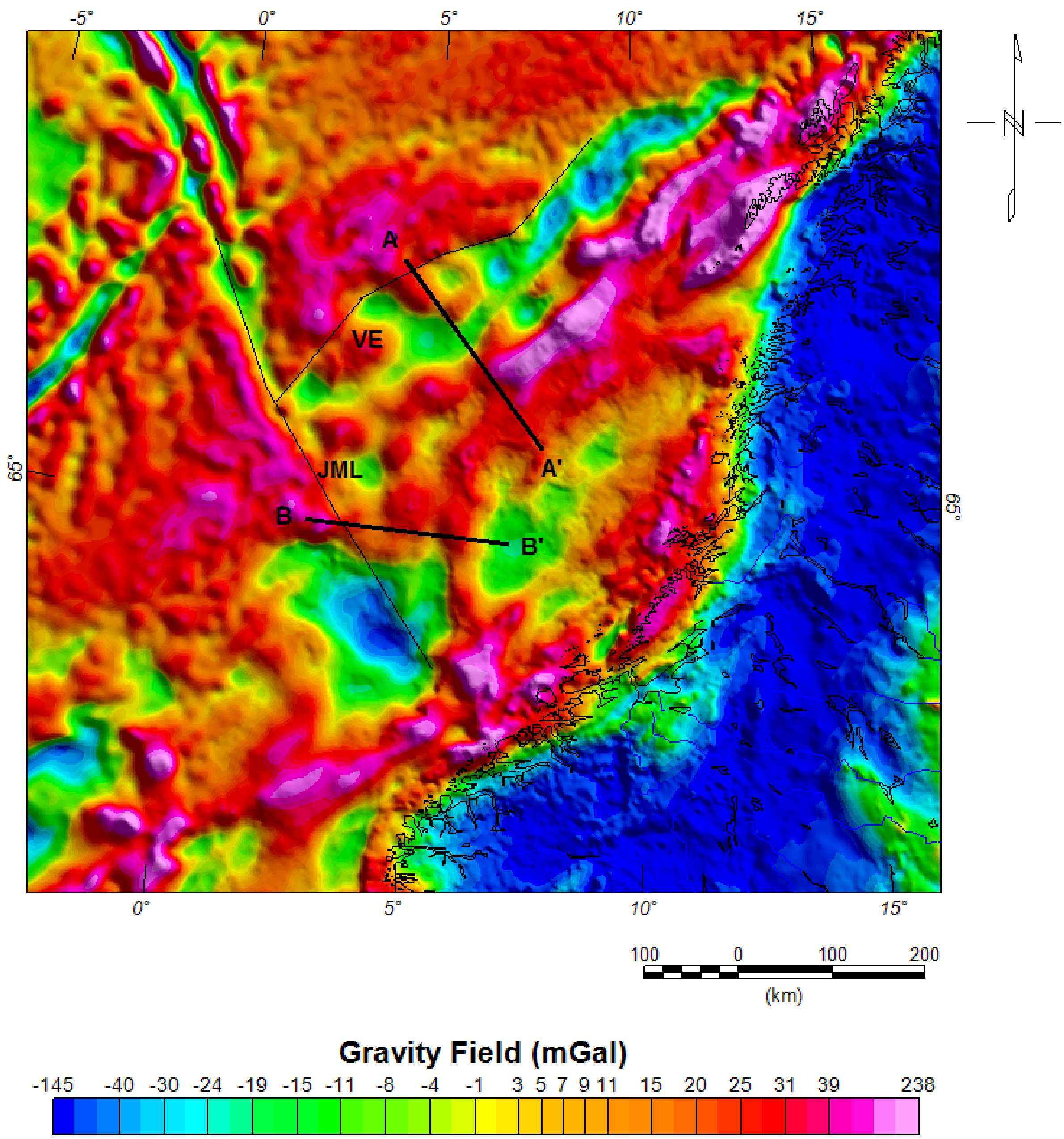

Figure 4.3: Gravity anomaly map of the study area, here with the Geoseismic transects AA' and BB' used for the seismic interpretation. The transects are shown in Fig.4.5. The gravity data is from the regional compilation of Olesen et al. [2010a,b]. JML: Jan Mayen Lineament; VE: Vøring Escarpment.

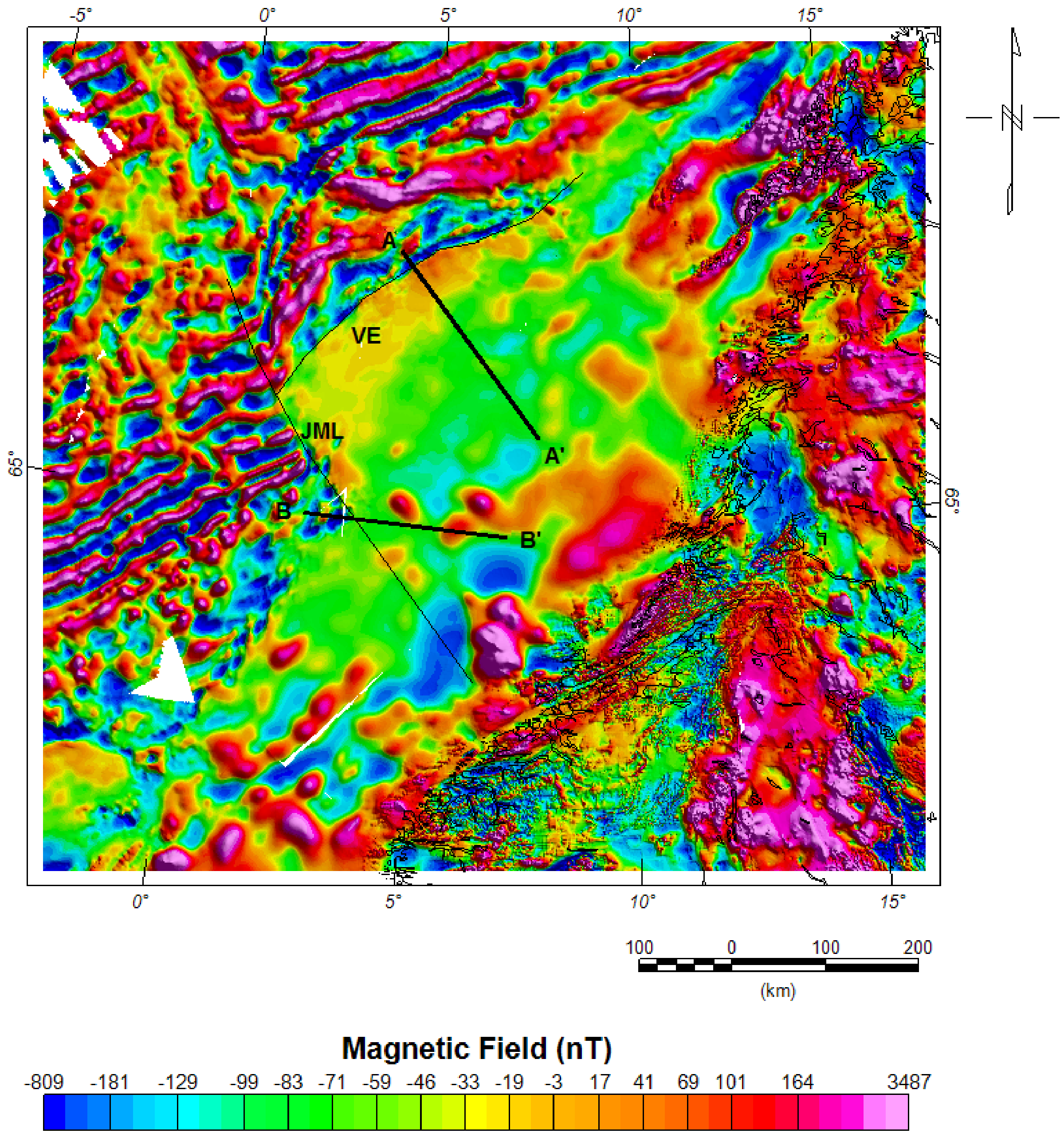

Figure 4.4: Magnetic anomaly map of the study area, here with the Geoseismic transects AA' and BB' used for the seismic interpretation. The transects are shown in Fig.4.5. The magnetic data is from the regional compilation of all pre-existing ship track and aeromagnetic data available. It has been published by Olesen et al. [2010a]. JML: Jan Mayen Lineament; VE: Vøring Escarpment.

ms. Two long-offset seismic lines have been studied in detail. As illustrated on Fig.4.1, line AA' is focused on the central part of the Vøring Margin crossing the Vøring Basin from the Dønna Terrace on the Trøndelag Platform in the east to the Vøring Marginal High in the north-western part of the margin; and line BB' crosses the Jan Mayen Lineament from the Halten Terrace in the southern part of the Vøring Margin to the Møre Marginal High of the northern part of the Møre Margin. The data is of good quality and provides an overview of the regional geology in the study area. Fig.4.5 shows two seismic sections used for the seismic interpretation, for location see Fig.4.1 - 4.4.

The refraction data used in this thesis is based on the previous publications of Mjelde et al. [2009a,b], Raum et al. [2002] and Breivik et al. [2011]. Fig.4.6 shows the structural map with location of the studied Transects AA' and BB' and nearby located published refraction profiles used in the thesis. The Transect A from Mjelde et al. [2009a] and Profile 10 from Raum et al. [2002] are located nearby the studied Transect AA'. The Profile 5-99 from Mjelde et al. [2009b], Profile 14 from Raum et al. [2002] and Profile 3-03 from Breivik et al. [2011] are located nearby the studied Transect BB'. The refraction profiles are shown in Fig.4.7 - 4.10.

The velocity information for the depth conversion and density information for the potential field modeling have been obtained through published deep seismic refraction data and wide-angle transects, illustrated on Fig.4.7 - 4.10.

Figure 4.5: Geoseismic sections AA' and BB'. See Fig.4.1 - 4.4 for the line locations. Seismic sections are in two-way traveltime (milliseconds).

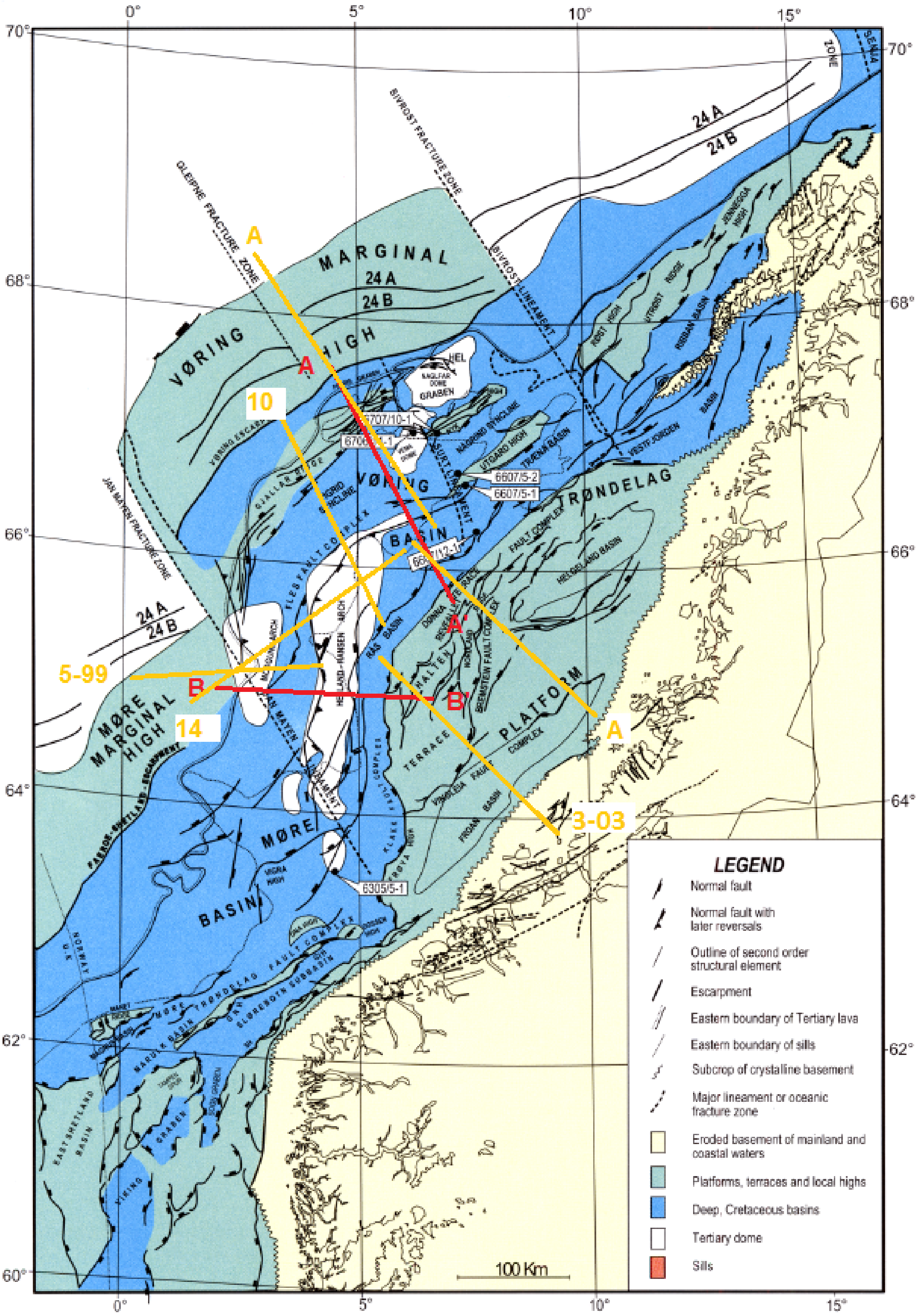

Figure 4.6: Structural map showing the location of the studied Geoseismic transects AA' and BB' (red) and nearby located refraction profiles (orange) from Mjelde et al. [2009a,b], Raum et al. [2002] and Breivik et al. [2011] which are used in the thesis. The Transect A and Profile 10 are located nearby the Geoseismic Transect AA'. The Profiles 5-99, 14 and 3-03 are located nearby the Geoseismic Transect BB'. The transects are shown in the Fig.4.7 - 4.10. Modified from Brekke [2000].

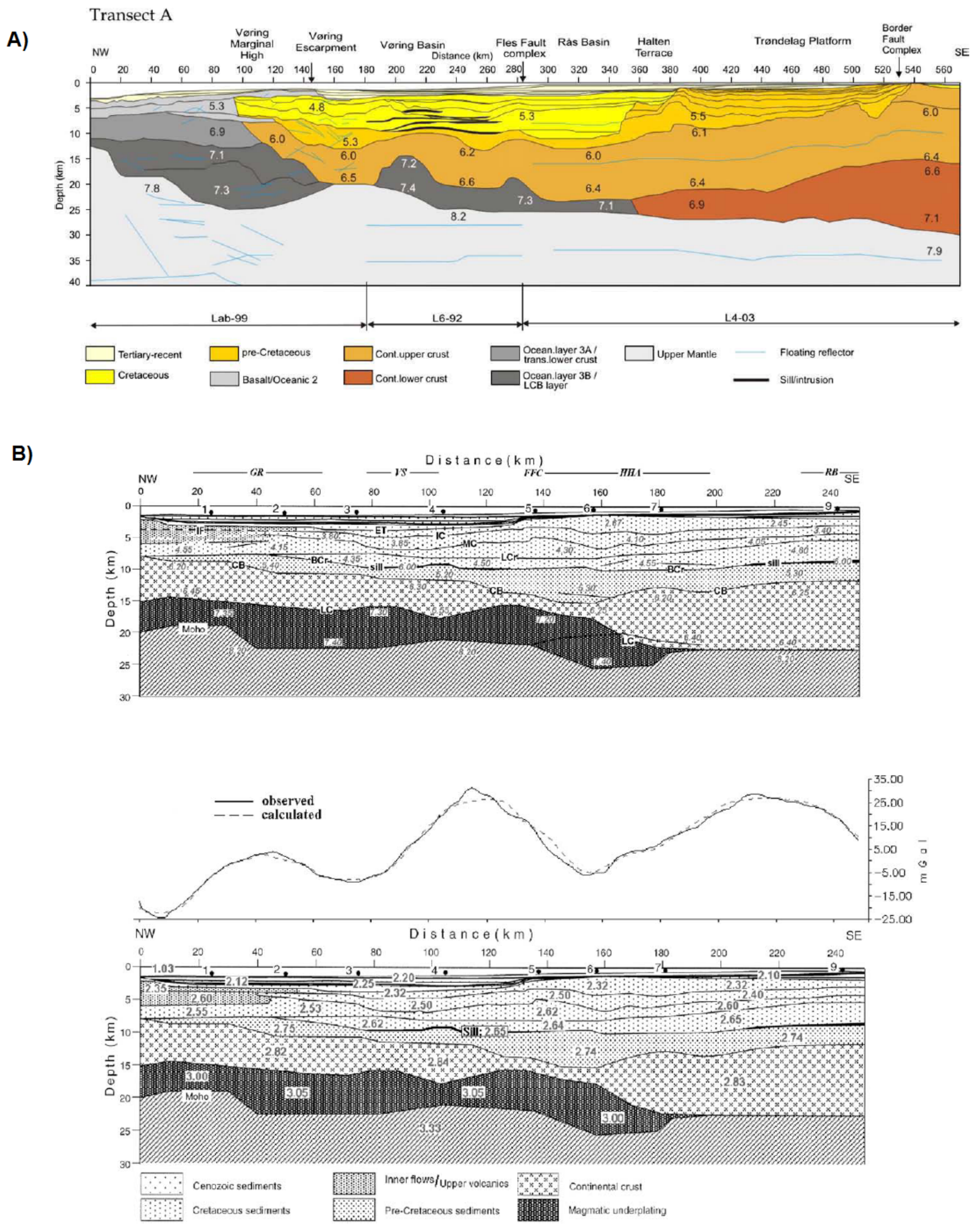

Figure 4.7: Refraction profiles located nearby the Geoseismic Transect AA'. See Fig.4.6 for the lines location. **A):** Transect A from Mjelde et al. [2009a]. Geological interpretation of velocities (assigned in the Profile in km/s) derived from the modeling of OBS data; **B) top:** 2D model for Profile 10 from Raum et al. [2002] with inferred P-wave velocity (in km/s); **B) bottom:** The corresponding 2D-gravity model with inferred densities (in g/cm3).

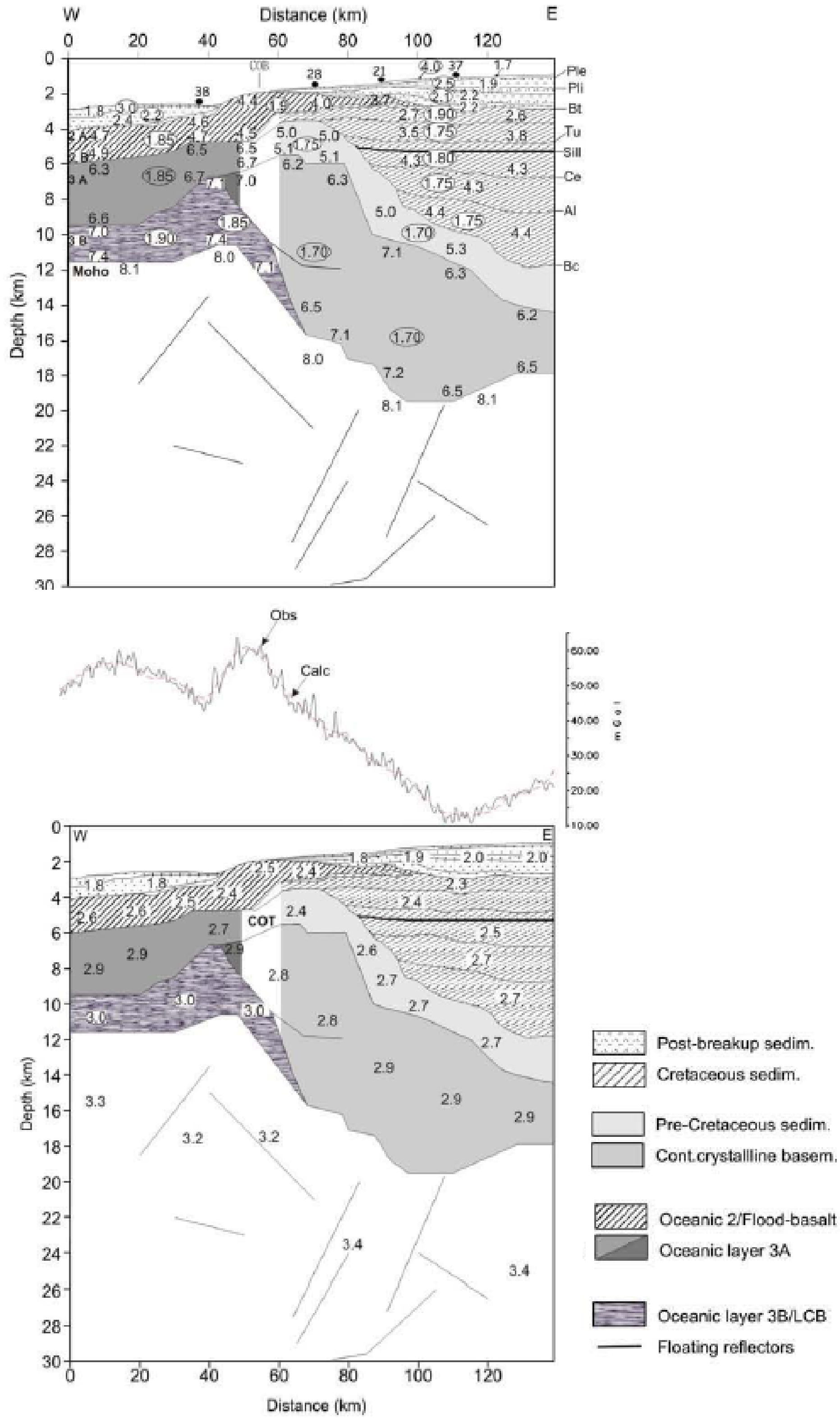

Figure 4.8: Refraction profile 5-99 from Mjelde et al. [2009b] located nearby the Geoseismic Transect BB'. See Fig.4.6 for the line location. **Top:** P-wave model, numbers are P-wave velocities in km/s and circled numbers are Vp/Vs-ratios; **bottom:** Observed and calculated free-air gravity anomalies, and the gravity model with inferred densities in g/cm3.

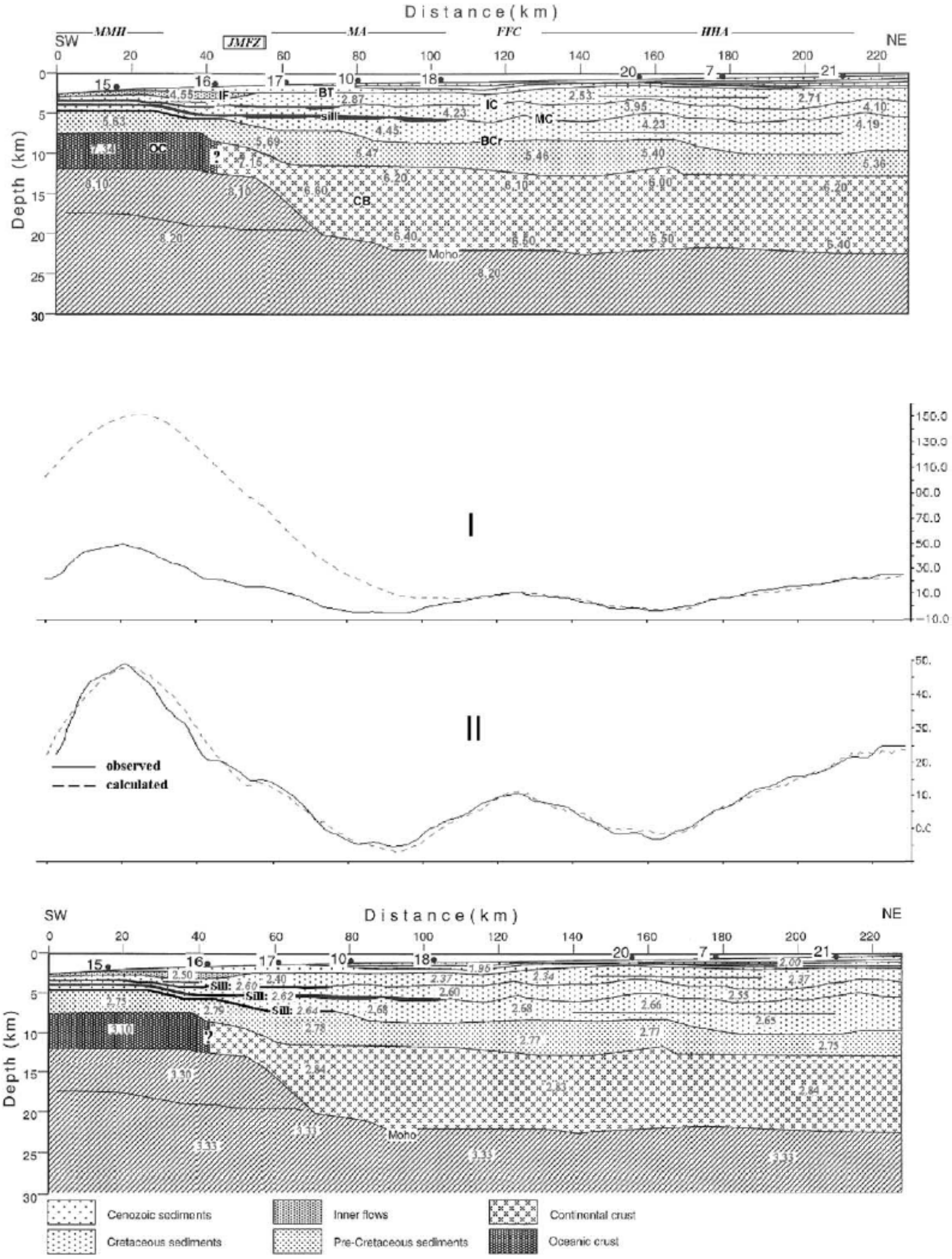

Figure 4.9: Refraction profile 14 from Raum et al. [2002] located nearby the Geoseismic Transect BB'. See Fig.4.6 for the line location. **Top:** 2D model with inferred P-wave velocities in km/s; **bottom:** The corresponding 2D-gravity model with inferred densities (in g/cm3). Clear misfit is observed in (I) between the two gravity curves as the profiles enters the Møre Marginal High.The fit between curves are gained in (II) considering the temperature effect.

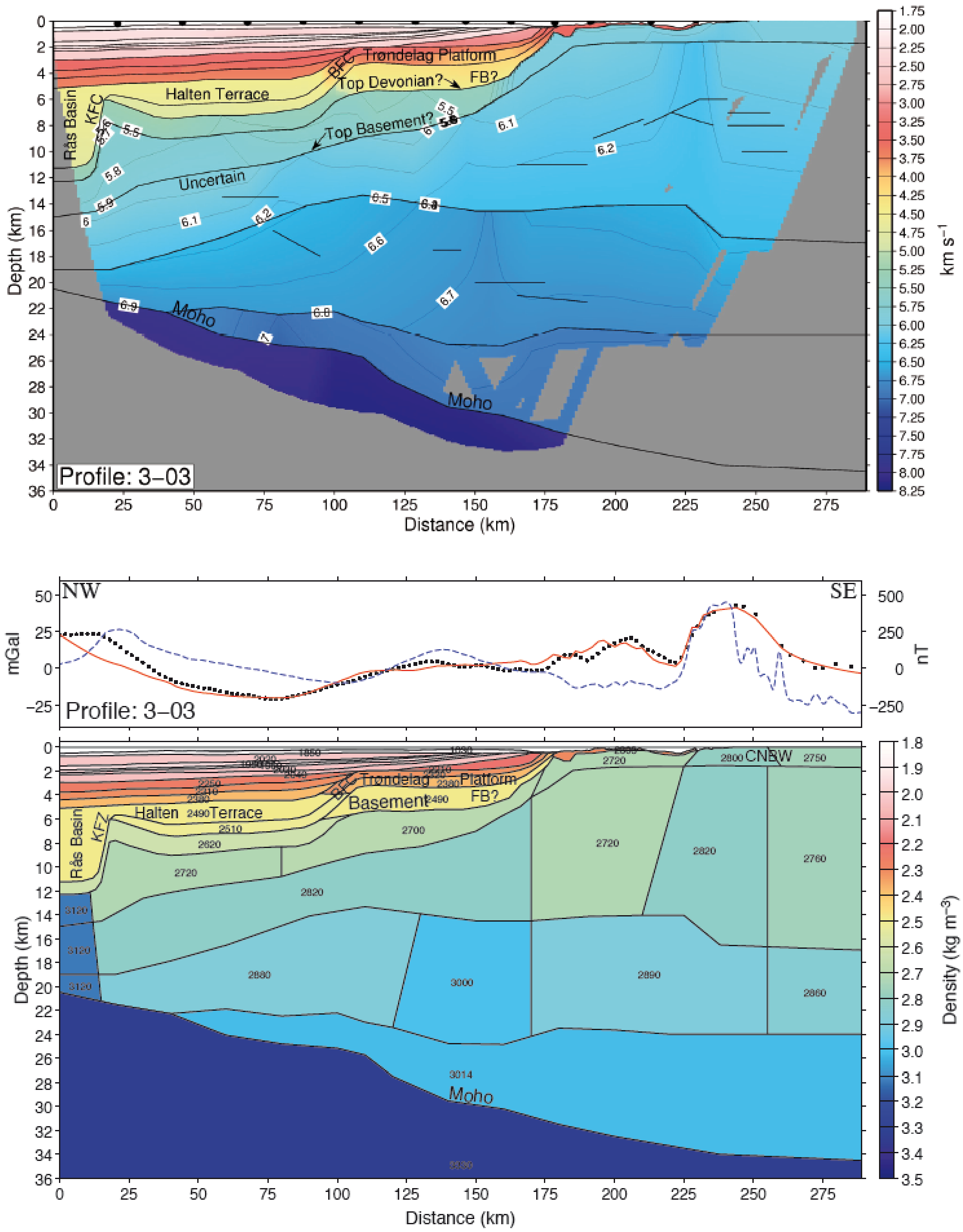

Figure 4.10: Refraction profile 3-03 from Breivik et al. [2011] located nearby the Geoseismic Transect BB'. See Fig.4.6 for the line location. **Top:** crustal velocity model (in km/s); contour interval within the basement is 0.1 km/s; **bottom:** Gravity model with proposed density distribution within the crust (in kg/m3). The panel: observed gravity (dots), calculated gravity (red line), magnetic anomalies (dashed blue line). BFC: Bremstein Fault Complex, CNBW: Central Norway Basement Window; FB: Froan Basin; KFC: Klakk Fault Complex.

5 Methodology

5.1 Main workflow

In order to propose an architecture and tectonic evolution of the Vøring and Møre rifted margins, forward modeling of the density structure and the magnetic properties of the crust in addition to seismic were used to model the crustal structure of continental margins.

Fig.5.1 shows the diagram outlining the thesis main workflow.

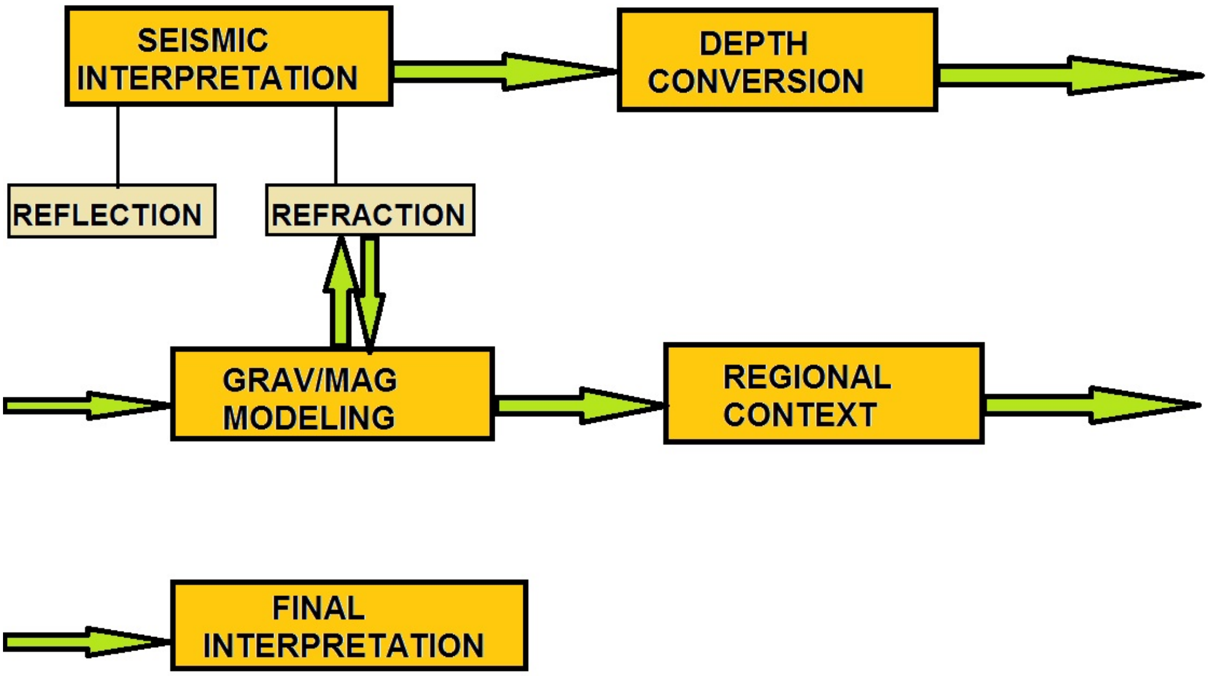

Figure 5.1: The diagram oultining the thesis main workflow.

Two seismic profiles shown on the Fig.4.5 have been interpreted with emphasis on the major features and crustal structures. Afterwards, the interpreted profiles have been depth converted and prepared for the forward modeling. The depth converted profiles have been used as input for the potential field modeling. The refraction data is based on the previously published modeling results (Fig.4.7 - 4.10). Using the seismic interpretation results with the final gravity/magnetic modeling results, it was possible to construct deep crustal transects along the profiles. Taking into account the regional settings and by comparing the results with earlier workers, margin configuration can be discussed in the regional context. The final interpretation of the results and conclusion is the last step of the main workflow.

5.2 Applied software

The software programs used in this thesis are listed in the Table 5.1.

Table 5.1: The software programs used for this thesis.

NO.	**Software program**	**Description /applied for**
1	TeXworks 0.4.3 r.857 (MikTeX 2.9)	Used to write the thesis
2	PETREL 2010.2.2	Seismic interpretation and depth conversion of the seismic sections
3	GEOSOFT 7.3 (JY) SP2	Map generation: bathymetry, gravity- and magnetic anomaly maps
3	GMSYS 7.3 (JY)	Modeling of profiles along the seismic lines

6 Results and discussion

In this chapter, a more detailed description of each step of the workflow will be given.

6.1 Seismic Interpretation

This section presents the results of seismic interpretation of two long-offset seismic lines shown on the Fig.4.5 (for location see Fig.4.1 - 4.4). The key profiles cover the main part of the continental margin - the line AA' is focused on the central part of the Vøring Margin, and the line BB' crossing the transition between the Møre and Vøring Margins. The seismic data is of good quality with nearly continuous reflectors with strong amplitude contrasts.

There are four fundamental horizons which are of particularly high interest: the Seabed, the Base Cretaceous Unconformity (BCU), the Top Crust and the Moho. The configuration of the deep structure of the margin from BCU further down into deeper levels can provide the geological input in the potential field model. To keep the main focus of the seismic interpretation in mind, the interpretation is divided into the main structural features part (from the Seabed down to the BCU) and the deeper crustal levels part (from the BCU further down into the deeper levels). The identification of the horizons and especially the faults are reliable at shallow depth, and more speculative to deeper levels of the basin.

6.1.1 Main structural features - from Seabed down to BCU

The geological evolution and structural settings of the Vøring and Møre Margins (Chapter 3), as well as the information provided by profiles from Brekke [2000] (Fig.3.6), Osmundsen et al. [2002] (Fig.3.7), Blystad et al. [1995], Faerseth and Lien [2002] are used as the starting point for the seismic interpretation of main structural features.

Profiles EE' and JL'L from Brekke [2000] (Fig.3.6), and Profiles 6 and 7 from Osmundsen et al. [2002] (Fig.3.7) are located nearby our studied key profiles AA' and BB'. They provide useful information about the succession and age of the main sedimentary sequences in the area and used as a first-order constraint to build a crustal structure of the margin.

It is important not to begin with a detailed interpretation but to have a full overview and understand the regional geological context. It is also important to pay attention to some seismic features which might lead to uncertainties in seismic interpretation (e.g. sills and multiples).

Different scenarios of interpretation have been carried out due to lack of well data and no possibility to tie well to seismic data.

The technique of seismic interpretation is to divide the seismic section into areas of common families and mark the boundaries where these families end. Identification of important reflectors and reflection terminations, as well as seismic sequences and unconformities, are important in order to predict sedimentary facies change, related depositional environment and/or tectonic events.

Fig.6.1 and 6.2 show the interpretation of the Geoseismic sections AA' and BB' with the names of all interpreted horizons.

The description of the first order interpretation is applicable for both Geoseismic sections.

The **Seabed** reflector is traced with a help of the "autotracking" option which works for laterally consistent horizons. The major patterns have been defined afterwards, proceeding with more and more details deeper to the BCU.

The reflector below the sea bottom represents change in depositional environment or tectonic event (Fig.6.1). It might be the **Base Quaternary.** The sequence below appears to be eroded and the new package deposited in the glacial environment of the Plio-Pleistocene period. The strata below were deformed and truncated by erosion, representing an angular unconformity. The underlying horizons terminate on the Base Quaternary unconformity reflector.

The horizon below might mark the **Top Eocene** which possibly reflects continuation of the pattern of post-rift subsidence at times, when the basin was influenced by opening of the Atlantic Ocean. More subsidence and sediment supply occured with westward progradation of the deltaic systems. The sediment package between the Base Quaternary and the Top Eocene consists of prograding clinoform reflection configurations with the downlap onto the Top Eocene horizon.

The reflector below is characterized by high amplitude reflection and could be followed through nearly all the key sections. The horizon possibly marks the **Top Cretaceous** event. The global sea level reached its maximum and the transgressive event could erode the succession and bring deep marine sediments, "tracing" the Top Cretaceous horizon by increased influx of clay in an open marine environment.

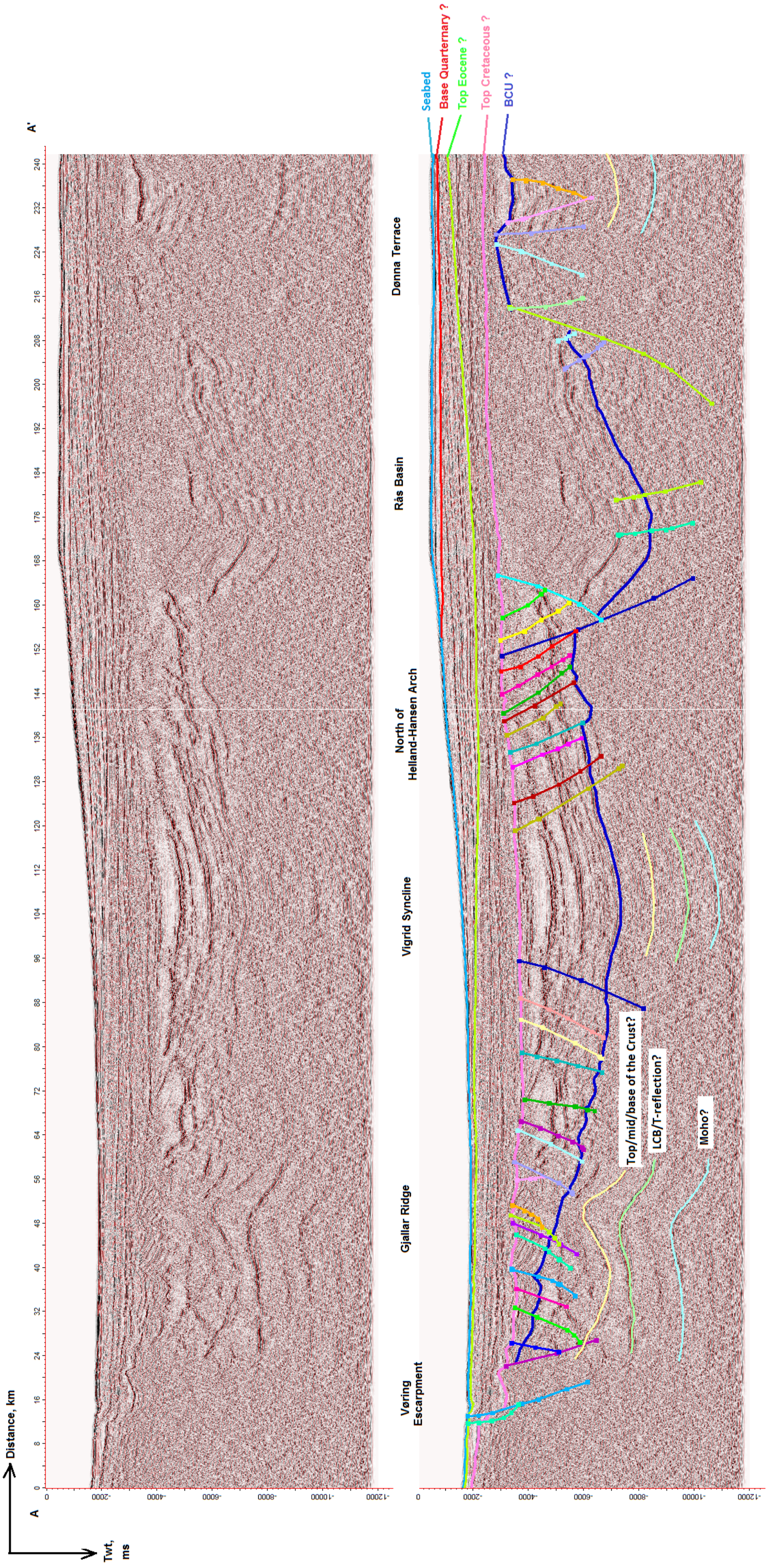

Figure 6.1: Seismic interpretation of the Geoseismic section AA'. See Fig.4.1 for the line location. Seismic section is in two-way traveltime (milliseconds). LCB: Lower Crustal Body (see text for details).

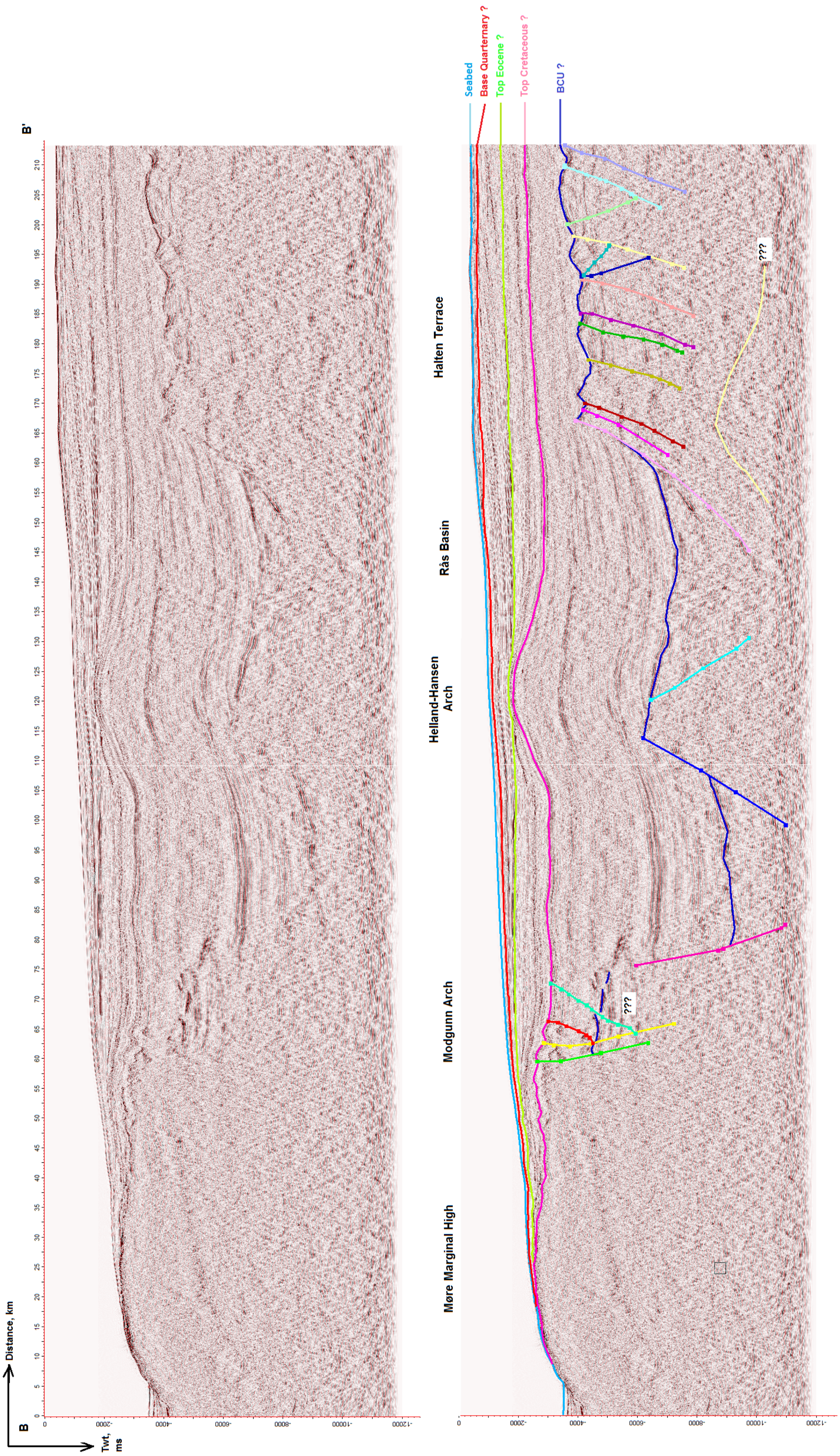

Figure 6.2: Seismic interpretation of the Geoseismic section BB'. See Fig.4.1 for the line location. Seismic section is in two-way traveltime (milliseconds).

6.1.2 Deep crustal levels - from BCU down to Moho

The deep crustal parts are difficult to map using seismic reflection method alone. The deep structures are poorly imaged due to the presence of flood basalts and sills in the western part of the Geosesmic Transects, and because of thick piles of sediments in the central basins.

Information about deep structures, e.g. the deep sedimentary structures, the top of the crystalline basement, the distribution of the lower crustal body (LCB) and the depth to Moho, has been obtained through published deep seismic refraction and wide-angle transects [Brekke, 2000; Blystad et al., 1995; Faerseth and Lien, 2002; Skogseid and Eldholm, 1987; Gernigon et al., 2003, 2004; Mosar et al., 2002; Osmundsen et al., 2002; Osmundsen and Ebbing, 2008; Raum et al., 2002; Mjelde et al., 2002, 2003, 2009a,b].

Base Cretaceous Unconformity

The BCU reflector in the Vøring and Møre margins is still a matter of some discussion. The unconformity lies deep within the basin areas and displays great local complexity and variability. Skogseid and Eldholm [1987] have placed the base Cretaceous at shallower depths west of the Fles Fault Complex. The minimum regional thickness of the pre-Cretaceous sedimentary sequence then has been estimated to be 3 km. However, Blystad et al. [1995] and Brekke [2000] have argued for a considerably thicker sequence of Cretaceous sediments and reduced thickness of the pre-Cretaceous sediments. The Cretaceous sedimentary infill is reported as being about 8-9 km in thickness [Osmundsen et al., 2002; Brekke, 2000; Brekke et al., 2001; Blystad et al., 1995] (Fig.3.6 and 3.7).

Throughout the interpretation, it was paid attention to the variations in the geometric configurations, occurance of onlap, downlap and the hiatus related to the unconformity. The Base Cretaceous is characterized by the culmination of many structural events in the basin. The subsidence and transgression caused erosion and marked this event with a significant hiatus.

Different scenarios for interpretation of the BCU in the **Geosesmic Transect AA'** have been carried out (Fig.6.1). The BCU reflector in the Rås Basin was previously traced at the shallower depth, between 5 and 6 s twt. After comparing the interpretation results with Brekke [2000] and Faerseth and Lien [2002], the BCU reflector was changed to the deeper depth of 6-8 s twt. The interpretation of Brekke [2000] is based on the updated exploration and scientific studies of the Norwegian-Greenland Sea from the Norwegian Petroleum Directorate (NPD). The author had reported the depth for the BCU reflector in the Rås Basin between 6 and 8 s twt. Faerseth and Lien [2002] based their interpretation on the well data from the deep basins, used further to support Norsk Hydro's seismic interpretation of two- and three-dimensional surveys in the study area. Faerseth and Lien [2002] proposed the depth for the BCU reflector in the Rås Basin up to 7 s twt, explaining the origin of the thick Cretaceous succession by interplay of different factors, e.g. increased sedimentation rate in the area, connection to a hinterland with a sediment source, increased regional subsidence rate etc. The thick Cretaceous deposits of the Rås Basin are separated by west-dipping fault from the thin Cretaceous sediments of the Dønna Terrace. The Cretaceous post-rift sediments onlap towards both sides of the basin.

The western part of the Transect AA' near the Vøring Escarpment is affected by sill intrusions. Therefore, important uncertainties in tracing of the BCU reflector remain in that part of the system.

Likewise to the Transect AA', the western part of the **Geoseismic Transect BB'** shows poorly imaged crustal structures, affected by sill intrusions (Fig.6.2). Due to ambiguity in the fault geometry and location of the BCU, the interpretation of the crustal structure in the Modgunn Arch area is left with a question mark.

The BCU reflector in the Dønna- and Halten Terraces in both Transects corresponds to a strong seismic marker as reported in several publications [Blystad et al., 1995; Brekke, 2000; Faerseth and Lien, 2002] and based on the Ocean Drilling Program (ODP) results.

The pre-Cretaceous sequences can be seen on seismic only on platforms and terraces landward of the basins [Brekke, 2000; Blystad et al., 1995; Zielger, 1988; Faerseth and Lien, 2002; Osmundsen et al., 2002] and are not traced throughout the basins due to poor seismic resolution.

Top Crust, Lower Crustal Body and Moho

The main concern and interesting feature of the **Geosesmic Transect AA'** is the mid-crustal dome-shaped high amplitude reflections, underlying the North Gjallar Ridge (Fig.6.1). Gernigon et al. [2003, 2004] studied the deep structures of the outer Vøring Basin with the emphasis on a high-velocity lower crustal dome marked by a strong amplitude reflection and named the T-reflection. Recent investigations suggest that the T-reflection coincides with the top of the continental part of Lower Crustal Body [Gernigon et al., 2003, 2004; Mosar et al., 2002]. The T-reflection is marked as the 'LCB/T-reflection?' on the Fig.6.1. Relying on the studies of the authors mentioned above, the reflectors might represent the top of a lens of lower crust, or an ultramafic body, or underplated material, or the Moho.

The mid-crustal reflections underlying the Vigrid Syncline might also represent the top/mid/base of the Crust, top/base of the LCB or the Moho. Gernigon et al. [2003] reported that the T-reflection (LCB) extends over a large part of the outer Vøring Basin and is limited to the east by the Fles Fault Complex interpreted as a major crustal boundary (Fig.4.1). It implies that the observed mid-crustal reflections underlying the Vigrid Syncline could be extended laterally from beneath the Gjallar Ridge towards the eastern part of the Transect.

There are two more mid-crustal reflections observed beneath the Dønna Terrace. These might represent the top/mid/base of the Crust or the Moho since the LCB/T-reflection has not been reported so far in this area.

The **Geoseismic Transect BB'** does not provide any information about positioning of deep interfaces due to poor seismic resolution of the deep crustal structures. However, the dome-shaped high amplitude reflection is observed beneath the Halten Terrace (Fig.6.2). Osmundsen et al. [2002] and Osmundsen and Ebbing [2008] studied the deep structure of the southern Vøring/northernmost Møre Basins. The antiformal structure with the crest located directly beneath the Bremstein-Vingleia Fault Complex (BVFC) (Fig.3.7 and 3.8) was observed under most of the Halten Terrace to c. 9,5 s twt before it was rising again slightly towards the Klakk Fault Complex (KFC), that separates the Halten Terrace from the southern Vøring Basin [Osmundsen et al., 2002]. The authors proposed that large-magnitude extension along a Palaeozoic detachment resulted in the formation and denudation of an antiformal, metamorphic core-complex in the southern Trøndelag Platform-Halten Terrace area. Based on the observations from Osmundsen et al. [2002] and Osmundsen and Ebbing [2008], the dome-shaped reflection observed beneath the Halten Terrace on the Geoseismic Transect BB' might represent the exhumed deep crust or subcontinental mantle, related to the isostatic denudation of the footwall or/and rotation on the Møre-Trøndelag Fault Complex.

6.1.3 Sills and low-angle dikes

Seismic data reveals that magmatic rocks, due to the early Tertiary continental break-up, were partially extruded on the surface as flood basalts and partially intruded as sills into the sedimentary Vøring and Møre Basins [Planke et al., 2000; Berndt et al., 2001].

Numerous sills and low-angle dikes are recognized east of the Møre- and Vøring Marginal Highs by most authors [Brekke, 2000; Blystad et al., 1995; Raum et al., 2002; Planke et al., 2000; Berndt et al., 2001].

The top and base of sills are expected to cause high amplitude reflections due to the high acoustic impedance contrast between intrusion and sediment. Sills also can cross-cut through the sedimentary layers. Sill reflections can be correlated to at least one nearby seismic section in order to avoid erroneous interpretation due to some side effects and coherent seismic noise (multiples, reflected refractions, processing inaccuracy). Continuity, which might be correlated to a number of other lines, and an abrupt termination without gradual thinning of the reflections, are additional criteria for interpretation of sills and low-angle dikes. In the westernmost Vøring and Møre Basins several sills and low-angle dikes seem to follow and/or cut the stratification causing the problem in identification of faults and correlation of the horizons (Fig.6.1 and 6.2).

6.1.4 Seismic interpretation problems

There are large uncertainties in the interpreted and stratigraphic geometries shown in Fig.6.1 and 6.2. Problems in identification of fault geometry and correlation of the main horizons, especially for the deep structures, are a consequence of lack of the well data, poor control of the stratigraphy in the deeper parts of the basins, significant erosion of the Top Cretaceous level, growth sequences, poor seismic resolution due to the presence of igneous features, which make individual seismic correlation extremely difficult in some places.

Seismic interpretation alone is not conclusive and additional method for the construction of the crustal structure is required. The potential field modeling further constrains the crustal structure of the continental margin.

6.2 Depth Conversion

The interpreted Geoseismic Transects (Fig.6.1 and 6.2) have to be depth converted and prepared for potential field modeling. Depth conversion allows the conversion of two-way time (twt) sections to geological depth-sections.

The first step in the depth conversion process is to create a Velocity Model. This Model is used as the input for the depth conversion.

For the Velocity Model, major horizons have been defined and the velocity values have been assigned to the different layers. The surfaces have been defined in the time domain and average velocities have been defined for each layer.

The velocity information has been obtained through published deep seismic refraction data and wide-angle transects, located near the studied key profiles (Fig.4.7 - 4.10). Fig.6.3 summarizes the velocity database and shows the velocity values derived from the modeling of OBS data [Mjelde et al., 2009a,b; Raum et al., 2002; Breivik et al., 2011] and values used in the study. The average value in the range is used for the Velocity Model. The interval velocity is assumed to be a constant for each zone.

The Velocity Model is used for the General Depth Conversion process.
The result of the depth conversion is shown in Fig.6.4 and 6.5.

The following step in the workflow is to revise the model by doing forward modeling of the crustal structure of the margin.

Layered media	P-wave velocity values [km/s] - Published in literature					Velocity values used in the study, [km/s]
	Raum et al., 2002 (Profile 10)	Raum et al., 2002 (Profile 14)	Mjelde et al., 2009a) (Transect A)	Mjelde et al., 2009b) (Profile 5-99)	Breivik et al., 2011 (Profile 3-03)	
Sea bed - Base Quaternary	1.85-1.95	1.86-1.96		1,7		1,85
Base Quaternary - Top Eocene	1.90-2.20	2,1		1,9		2
Top Eocene - Top Cretaceous	2.20-2.80	1.95-2.25		2,2		2,3
Top Cretaceous - Base Cretaceous	2.45-4.50	2.87-4.45	4.8-5.3	2.6-4.4		3,5
Base Cretaceous - Crystalline Basement	5.20-5.40	5.36-5.69	5,5	5.00-5.30		5,3
Crystalline Basement - LCB	6.20-6.55	6.00-6.50	6.00-6.60	6.20-7.20	Top Basement-Moho: 6.1-7	6,4
LCB - Moho	7.20-7.40	7,34	7.10-7.40	7.00-7.40		7,25
Moho - further down	8,2	8,2	7.80-8.20	8.00-8.10		8,1

Figure 6.3: The values of P-wave velocity derived from the modeling of OBS data and published by Mjelde et al. [2009a,b], Raum et al. [2002] and Breivik et al. [2011]. The average values from the range are used for the Velocity Model. The interval velocity is assumed to be a constant for each zone.

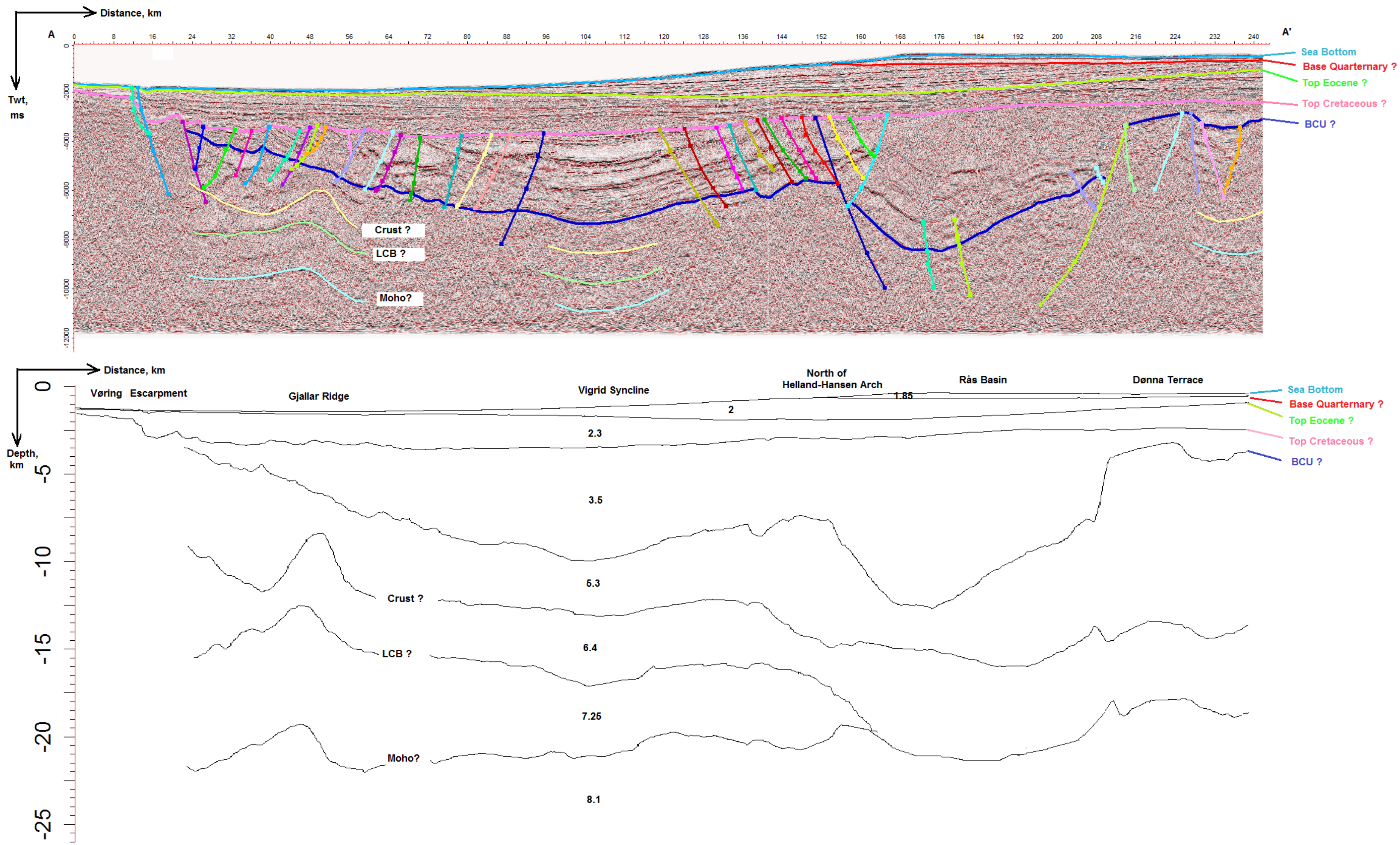

Figure 6.4: The interpreted in twt (ms) (on the top) and depth converted (on the bottom) Geoseismic section AA'. See Fig.4.1 for the line location. The assigned P-wave velocities (in km/s) for each zone are indicated in the depth converted section. LCB: Lower Crustal Body/T-reflection.

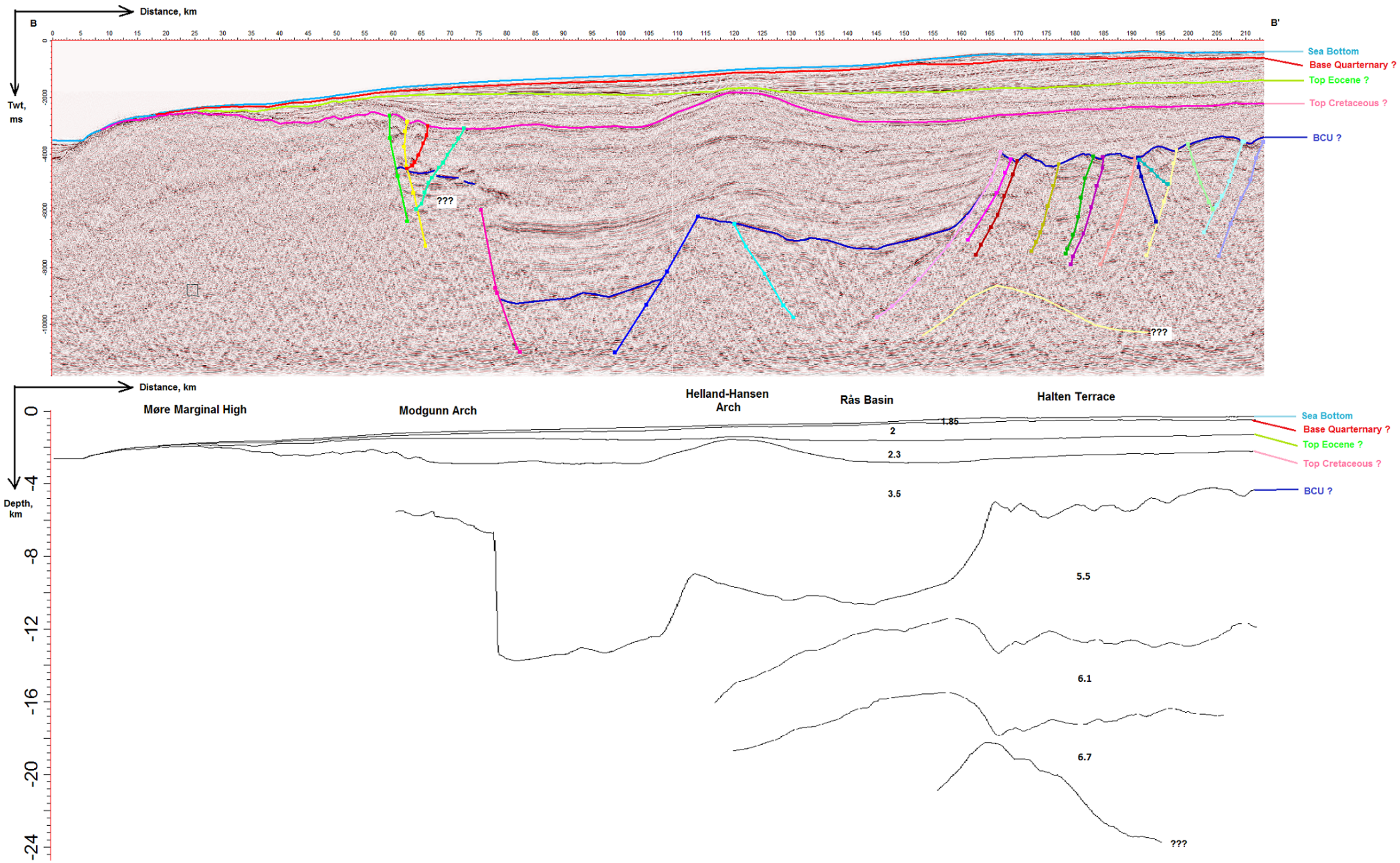

Figure 6.5: The interpreted in twt (ms) (on the top) and depth converted (on the bottom) Geoseismic section BB'. See Fig.4.1 for the line location. The assigned P-wave velocities (in km/s) for each zone are indicated in the depth converted section.

6.3 Potential Field Modeling

In this study the modeling program GM-SYS in linked mode within OASIS montaj program has been used. It enables to test the geologic model accuracy by comparing the calculated model's gravity and magnetic response to observed measurements. Both gravity and magnetic responses are calculated for the same geologic model.

The model consists of water, sediments, crystalline crust, LCB, igneous rocks and mantle which extends to a depth of 30 km. Based on the seismic data, the sediments are subdivided into the Cenozoic, Cretaceous and pre-Cretaceous units. Depth converted horizons of the Top Cretaceous and BCU unconformities provide geometrical constraints for the main sedimentary structures. The igneous rocks correspond to the lava flows at the Marginal Highs and sills and low-angle dikes in the basins.

The total normal magnetic field on the mid-Norwegian margin is assumed 51693.8 nT, an inclination of 74.58 ° and declination of 0.12 °.

Each model body was assigned a density, susceptibility and magnetic remanence.

Density and magnetic properties used for the modeling are based on the literature values from Raum et al. [2002], Mjelde et al. [2009a,b] and Peron-Pindivic et al. [2012a,b].

Fig.6.6 summarizes the petrophysical database used in the study.

Layered media	Densities [kg/m^3] - Published in literature			Density values used in the study, [kg/m^3]	Magnetic parameters used in the study (from Peron-Pindivic et al., 2012)		
	Raum et al., 2002	Mjelde et al., 2009	Peron-Pindivic et al., 2012		Susceptibility, SI	Remanence, A/m	Koenigsberger ratio Q
Water	1030	1030	1030	1030	0	0	
Sediments:							
Cenozoic	1950-2250	1800-2200	2100	2100	0,001	0	
Cretaceous	2400-2650	2500-2700	2560	2500	0,001	0	
pre-Cretaceous	2740-2750	2700-2800		2740	0,001	0	
Crust:							
Upper	2820-2840	2800-2900	2740	2820	0,005	0	
Lower	2820-2840	2800-2950	2950	2950	0,005	0	
LCB	3000-3120	3000-3200	3050	3050	0,01	from -0.5 to +0.5	
Mantle:							
Subcontinental	3300-3340	3300	3300	3300	0,001	0	
Attenuated			3100	3100	0.001	0	
Flood basalts	2650		2600	2650	0,01	from -0.3 to +0.5	0.7 - 1.1

Figure 6.6: Petrophysical properties published and applied in the model. Properties of the crust are based on the previous modeling and petrophysical studies in the area from Peron-Pindivic et al. [2012a,b], Raum et al. [2002], Mjelde et al. [2009a,b].

The forward model calculation is divided into three steps. First, a simple model constructed out of the available depth converted seismic data. Second, the gravity and magnetic signals are calculated and compared with the observed anomalies. Finally, the model is changed in order to improve the correspondence between the observed and calculated anomalies.

6.3.1 Step 1 - based on the seismic data

In order to determine the deep crustal architecture across the Vøring and Møre Basins, a crustal model was constructed based on the interpreted sections AA' and BB'. Subsequently, the blocks shown in the Fig.6.7 and 6.8 were created keeping the upper crustal geometries fixed.

As the Step 1 is based only on the seismic interpretation results, the lower crustal geometries along the Geoseismic Transect BB' are more simplified because of lack of information about positioning of deep interfaces due to poor seismic resolution.

A starting point for the modeling of the lower crustal geometries was based on the following studies.

As introduced, the **pre-Cretaceous sequence** is difficult to interpret due to poor seismic resolution. Skogseid and Eldholm [1987] estimated the thickness of the pre-Cretaceous sediments to be ca. 3 km west of the Fles Fault Complex, while Blystad et al. [1995] and Brekke [2000] have argued for reduced thickness of the pre-Cretaceous package. The only well established pre-Cretaceous sequences are resolved on the platforms and terraces landward of the basins [Brekke, 2000; Blystad et al., 1995; Zielger, 1988; Faerseth and Lien, 2002]. Based on the studies mentioned above, the minimum regional thickness of the pre-Cretaceous sequence in the model is assumed to be 2-3 km and around 5 km on the Dønna and Halten Terraces.

Ebbing et al. [2006] reported the depth of **Top Basement** to be less than 9 km at the Trøndelag Platform and between 11 and 15 km below the Vøring Basin. Through modeling of high-quality OBS data, Mjelde et al. [2009b] and Raum et al. [2002] shown the thickness variation of the crystalline layer between 3 and 11 km with the general trend of crustal thinning basinwards. The basement shallows and thickens landwards, while basinward all profiles show crustal thinning with the most pronounced thinning west and south of the Helland Hansen Arch [Raum et al., 2002] (Fig.4.7). In agreement with crustal models along the margin from Raum et al. [2002], Mjelde et al. [2009a,b] and Ebbing et al. [2006], the depth of the Top Basement is assumed to be ca. 8 km at the Dønna and Halten Terraces and from 10 to 15 km below the Vøring and Møre Basins.

The observed on the Geoseismic Transect AA' dome-shaped feature above the assumed LCB/T-reflection (Fig.6.1) allows to subdivide the **Crust** into subunits of the Upper and Lower Crust, in order to account for increase in density with depth.

The occurrence of high velocities (7.1-7.8 km/s) **Lower Crustal Bodies (LCB's)** have been recognized for a long time along the NE Atlantic basins [Gernigon et al., 2004, 2006; Osmundsen and Ebbing, 2008; Ebbing et al., 2006; Raum et al., 2002; Mjelde et al., 2002, 2003, 2009a,b]. The LCB's are commonly interpreted as magmatic underplating that could be formed by magmatic material trapped beneath the Moho, or magmatic sills injected into the lower crust [White and McKenzie, 1989]. However, Gernigon et al. [2006] explained the LCB's by the presence of pre-existing high-velocity rocks, such as eclogites or migmatites, while Ebbing et al. [2006] proposed that the LCB could represent remnants of the Caledonian root. Peron-Pindivic et al. [2012b] proposed a nature of the

LCB beneath the basin as a combination of lower crustal (mafic/felsic?) lithologies and possibly serpentinized mantle, rather than pure magmatic material. The LCB's have been observed and modeled along the ocean/continent transition with some extension beneath the continental part of the crust. Mjelde et al. [2009a,b] suggested the maximum thickness of the LCB beneath the Møre Marginal High about 5 km, and about 8 km beneath the Vøring Marginal High (Fig.4.7 (A) and 4.8). Raum et al. [2002] proposed the variation in thickness of LCB from 2-3 up to 6-7 km (Fig.4.7 (B) and 4.9) and outlined the landward termination of the LCB beneath the Helland-Hansen Arch along the profile located nearby the Geoseismic Transect AA' (Fig.4.7 (B)). Considering this, the LCB in the model for the Geoseismic Transect AA' was assumed to occur between mantle and lower crustal rocks, extending laterally from beneath the Helland-Hansen Arch towards the Vøring Marginal High.

Raum et al. [2002] reported the depth to the **Moho** to be generally 20-23 km at the landward part with decreasing depth seawards to approximately 15 km. At this stage, it was assumed to keep the Moho uniform with homogeneous mantle below the crust. The dome-shaped high-amplitude reflection observed beneath the Halten Terrace on the Geoseismic Transect BB' (Fig.6.2) is assumed to correspond to Mantle rocks due to the deep positioning (about 20 km depth). The block between the pre-Cretaceous and Mantle surfaces is assumed to be crustal rocks with average density value of 2900 kg/m3 and susceptibility of 0.005 SI.

6.3.2 Step 2 - Gravity and magnetic anomalies: calculated vs. observed

The gravity and magnetic signals were calculated and compared with the observed anomalies.

Gravity and magnetic anomaly maps with location of the Geoseismic Transects AA' and BB' are shown in the Fig.4.3 and 4.4. Gravity and magnetic anomalies contain different wavelengths because of the different distances to the sources. Magnetic data provides information about the upper part of the crust, below the Curie temperature, where rocks generate magnetic signals. The limit depth between magnetic and nonmagnetic material generally runs at lower crustal levels. Sediments are relatively nonmagnetic, while the underlying basement and intrusive rocks have a high magnetic susceptibility [Ebbing et al., 2006]. The main sources of the magnetic field on rifted margins are therefore upper and top basement and intra-sedimentary volcanic rocks.

The observed gravity field is caused by the density distribution in the lithosphere. Because of the small density contrast between the deep sediments and the top basement (due to high sedimentary compaction at depth), the gravity field rarely includes a signal for the top basement. Hence, it is the magnetic signal that is used to constrain the top basement geometry [Ebbing et al., 2006].

Fig.6.7 shows the 2D model based only on the seismic interpretation of the **Geoseismic Transect AA',** assuming homogeneous mantle below the crust and without taking into account magmatic material with intrusions. The misfit between calculated and observed magnetic and gravity anomalies can be observed. Clear misfit is observed between the two magnetic curves as the profile enters the Vøring Marginal High, where magmatic material with different magnetic properties is not taken into account. General trend of fitted observed and calculated magnetic anomalies shows the correlation between the crustal geometry and magnetic interpretation.

Fig.6.8 shows the 2D model based only on the seismic interpretation of the **Geoseismic Transect BB'.** Like in the previous model, it was assumed the homogeneous mantle below the crust and no LCB and magmatic material with intrusions are taken into account, as they were not observed on the seismic. The misfit between observed and calculated anomalies is much greater than in the model for the Geoseismic Transect AA'.

The constructed simple models based on the available seismic data show clear misfit of observed and calculated gravity and magnetic anomalies. In order to find the relation between observed and calculated anomalies, the models had been improved further.

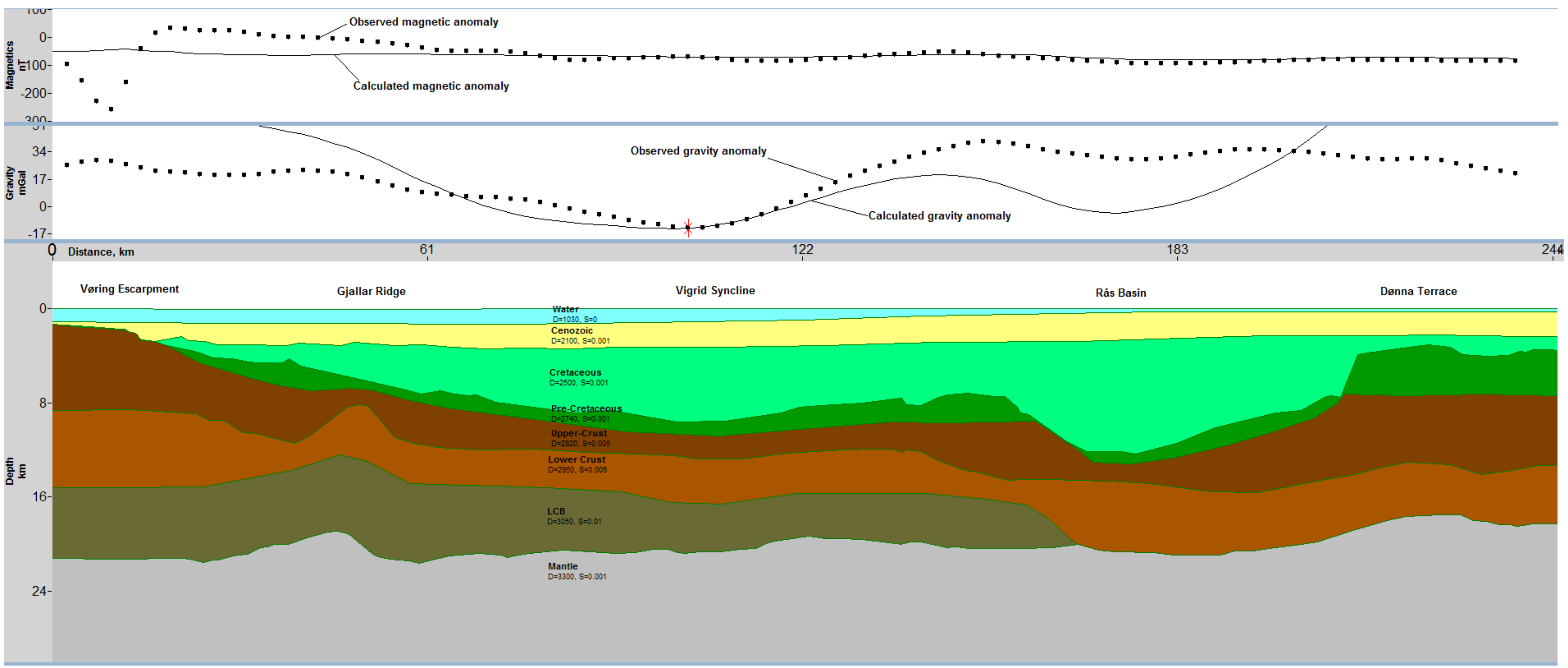

Figure 6.7: 2D model for Geoseismic Transect AA' based on the seismic interpretation results. The inferred petrophysical properties are indicated with densities (D) in kg/m3 and susceptibilities (S) SI. Clear misfit is observed between observed and calculated magnetic and gravity anomalies. See Fig.4.1 - 4.4 for the Transect location.

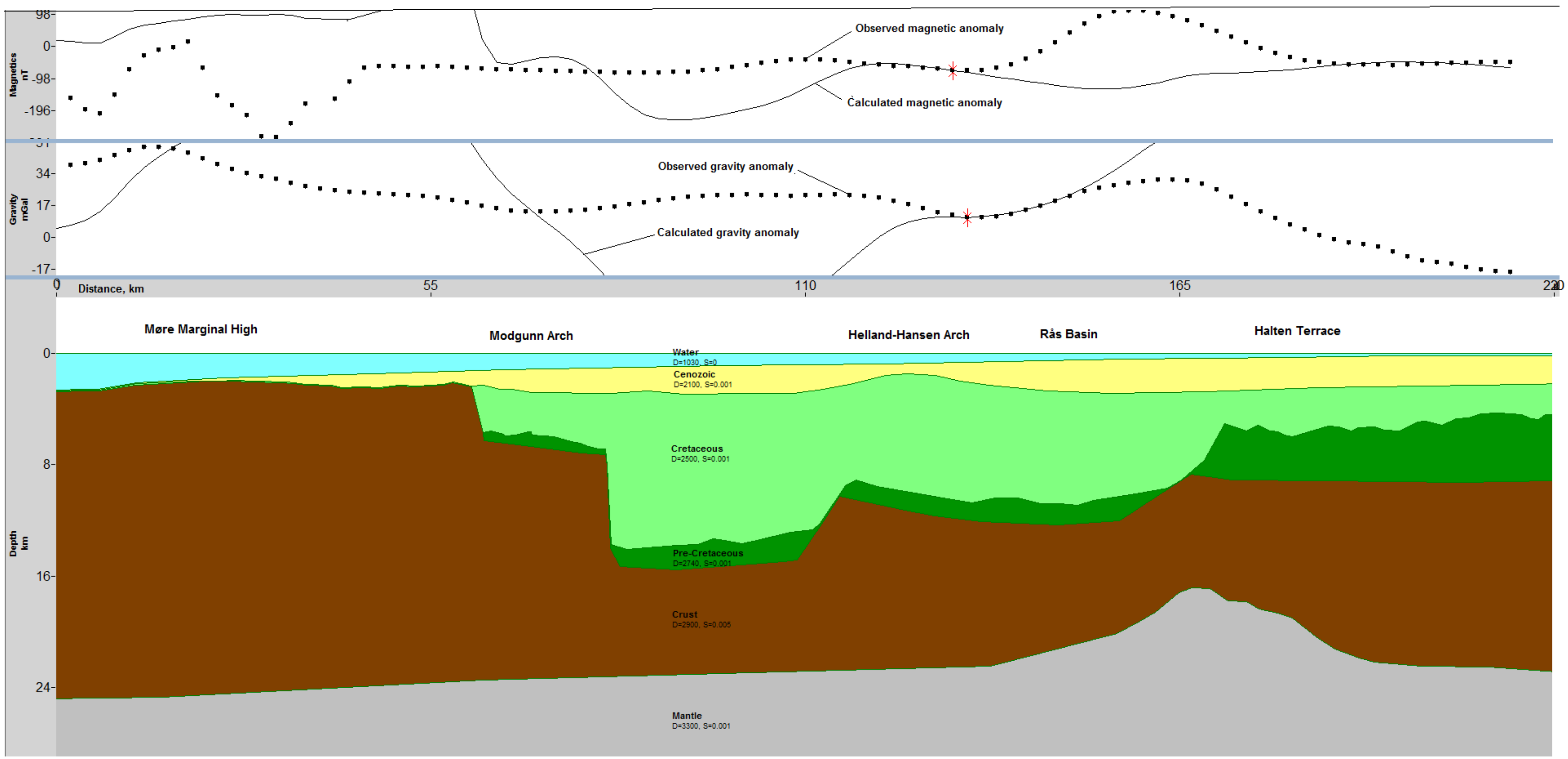

Figure 6.8: 2D model for Geoseismic Transect BB' based on the seismic interpretation results. The inferred petrophysical properties are indicated with densities (D) in kg/m3 and susceptibilities (S) SI. Clear misfit is observed between observed and calculated magnetic and gravity anomalies. See Fig.4.1 - 4.4 for the Transect location.

6.3.3 Step 3 - improving the model

In the following section, the models have been tested in order to evaluate the configuration of the deep crustal structure and the lithospheric mantle beneath the margin.

As introduced, the evolution of the NE Atlantic margin has been discussed for years. Brekke [2000] reported several minor phases of tectonic activity in the Cretaceous and Tertiary evolution of the Vøring Basin, while in contrast to the Vøring Basin, the Møre Basin has been tectonically quiet after the Mid-Jurassic - Early Cretaceous rifting. Faerseth and Lien [2002] argued in favour of Cretaceous tectonic quiescence of the Vøring Basin until the Early Campanian rifting.

Alternative scenarios are proposed by Osmundsen and Ebbing [2008] and Peron-Pindivic et al. [2012b]. These authors propose that the distal Vøring and Møre margins can be interpreted as deep sag-type basins with ongoing thinning of the margin. The authors support the scenario in which the formation of the sag basins correspond to periods of high tectonic activity during most of the Cretaceous times, accomodated by major detachment plans. The sag-type basins are interpreted as structurally developed by different tectonic processes and distinguished from the basins on the platform and terrace domains by overprinted tectonically developed deformation.

Fig.6.9 and 6.10 shows the final 2D models for the Geoseismic Transects AA' and BB'. Concerning different interpretations of the Vøring and Møre margins, the nature of the marginal high, the basement, the oceanic crust, the continent-ocean transition (COT) and the mantle have been further discussed below.

Marginal High

The nature and origin of the marginal high are highly complex and have been discussed for years. Due to the blanketing effect of intrusions and lava flows, it is very difficult to construct its deep structure.

The marginal high was described as consisting of subaerial and submarine basalts with abundant intrusive complexes in the sedimentary sequences of the Vøring and Møre Basins. Brekke [2000] reported that the Vøring and Møre Marginal Highs comprise Tertiary sediments on top of thick Lower Eocene flood basalts, which are probably underlain by continental crust that becomes transitional to oceanic crust towards the west. Blystad et al. [1995] reported that the marginal high has two zones with different structural development beneath the top Eocene lava reflector. The eastern zone forms a 10 to 40 km wide area west of the Vøring Escarpment and 15 to more than 100 km wide area west of the Faeroe-Shetland Escarpment, with nearly parallel to the top Eocene lava reflectors, representing lavas and volcanoclastics (ODP well 642). The lavas overlying Mesozoic or Palaeozoic sediments above continental or transitional crystalline crust. The western zone is underlain by a seaward-dipping reflector sequence (SDRs) representing a westward thickening lava pile which is the upper part of thick oceanic crust. The marginal high is described by Planke et al. [2000, 2005] and Berndt et al. [2001] as a magmatic complex comprising lava flows, lava deltas, seaward dipping reflectors (SDRs), intrusions and volcanic mounds.

In order to account for the flood basalts and intruded numerous sills and low-angle dikes in the basin [Brekke, 2000; Blystad et al., 1995; Raum et al., 2002; Mjelde et al., 2009a,b; Planke et al., 2000; Berndt et al., 2001], the Vøring and Møring Marginal Highs were modeled with a lens of flood basalts sandwiched between the Tertiary and Mesozoic sediments, with some extension towards the basin.

The Mesozoic sediments in the highs were assumed to be thicker, highlighting locally a deeper top-basement and shallower Moho than that was previously proposed (discussed further) [Peron-Pindivic et al., 2012b].

In agreement with Mjelde et al. [2009a,b] and Raum et al. [2002] (Fig.4.7), the LCB beneath the Vøring Marginal High has been modeled widespread with the thickness of ca. 5-8 km. However, the refraction studies in the Møre Marginal High tend to question the effective presence of such a widespread LCB there [Mjelde et al., 2009b] (Fig.4.8). The LCB in the Møre Marginal High was included as a a small lens with the thickness of ca. 2-3 km.

Oceanic crust and COT

Following the interpretation of Mjelde et al. [2009a,b] (Fig.4.7 A) and 4.8) and Raum et al. [2006], the oceanic crust below the Cenozoic sediments has three-layered structure. The upper layer 2AB is interpreted to consist mainly of flood basalts and diabase dikes, the middle layer 3A is assumed to be a mixture of sheeted dykes and gabbroic intrusions, and the lowest oceanic layer 3B has the properties of gabbros and ultramafic rocks.

The position and definition of the continent-ocean transition (COT) is uncertain in deep-rifted margins. Raum et al. [2006] defined the COT as the part of the lithosphere between the thinned continental crust characterized by tilted fault blocks and oceanic crust formed by seafloor spreading. They reported that the width of the COT varies considerably from 10 to 30 km.

The presence of the oceanic crust and COT can not be clearly resolved along the studied Geoseismic Transects, since the profiles terminate within the escarpment area. Fig.4.1 shows that the first identified magnetic spreading anomaly 24B located outside of the studied Geoseismic Transects. According to the definition of Blystad et al. [1995], the anomaly is characteristic of the oceanic crust. However, Raum et al. [2006] and Mjelde et al. [2009b] reported a well established velocity transition from continental to oceanic crust as the profiles in Fig.4.8 and 4.9 cross the Jan Mayen Fracture Zone. The increase is interpreted as being related to the Møre Marginal High, where the crust mainly is of oceanic character.

Considering limited extend of the studied Geoseismic Transects towards the west, it was decided not to take into account the oceanic crust and COT. Additional regional data are needed to resolve this issue.

Moho and upper mantle

In order to extrapolate the Moho distribution, Peron-Pindivic et al. [2012a] generated a gravity Moho map by 3D inversion of the free air gravity field. The map highlights the general deepening of the gravity Moho from beneath both marginal highs towards the continent, from ca. 12 km to 32 km. An anomalously shallow Moho have been reported in the south-western part of the Vøring Basin and beneath the Møre Marginal High. Modelling of OBS data acquired in the southern part of the Vøring Basin indicated ca. 5 km shallowing of the Moho southwards, without signs of related crustal subsidence [Raum et al., 2002; Mjelde et al., 2009b] (Fig.4.8 and 4.9). The detachment faulting has been proposed in order to explain both uplift of Gjallar Ridge, the intra-crustal T-reflector and the anomalously shallow Moho [Gernigon et al., 2003, 2004; Mjelde et al., 2003].

The depth to the Moho near the Vøring Escarpment has been reported of being ca. 20 km (Fig.4.7). Van Wijk et al. [2004] reported local crustal thickening beneath the Vøring

Marginal High with the maximum uplift, explained by large lateral thermal variations in the lithosphere at the onset of extension.

In agreement with the following investigations, the Moho depth beneath the Møre Marginal High for the Transect BB' was assumed of being ca. 12 km and ca. 20 km beneath the Vøring Marginal High with local crustal thickening.

The nature of the mantle has also been the topic for discussion. Recent studies show the highly complex density structure of the mantle than that of being proposed before. Based on the 3D gravity modeling results, Maystrenko and Scheck-Wenderoth [2009] stated a significantly lower density in the mantle below the ocean than below the continent with a possible relation to difference of thermal or compositional conditions beneath the two domains. Mjelde et al. [2009b] reported that the upper mantle density is 0.1 g/cm3 smaller in the oceanic domain compared with the continental part. Peron-Pindivic et al. [2012b] reported the presence of the attenuated mantle below the highs. The attenuated mantle is considered to be affected by tectonic and geochemical processes which changed its geophysical characteristics: might be highly deformed, serpentinized and magmatically infiltrated. The authors interpreted the basement constitutive of the Vøring and Møre Highs to be made of exhumed serpentinized mantle with remnants of undifferentiated continental crust, either as slivers sandwiched in between the detachment structures, or as allochthons.

Based on the studies mentioned above, the less dense mantle towards the oceanic domain has been included in the model.

Maystrenko and Scheck-Wenderoth [2009] reported an existence of isolated high-density zones (3110 kg/m3) incorporated in the lower continental crust beneath the Vøring Basin. The bodies form narrow structure below some structural highs of the crystalline basement. According to the thickness map of the high-density zones within the continental crust, the body beneath the Rås Basin and Halten Terrace can reach ca. 6 km in thickness. A high-density body has been included in the model for the Transect BB' corresponding geometrically to the body observed in the deep seismic data beneath the Halten Terrace.

Potential field modeling results

The modeling was carried out by interactive changes in the geometry and properties of the layers.

Fig.6.9 and 6.10 show that a good fit is obtained with the observed gravity and magnetic data after applying some modifications.

The following summarizes the main results regarding the correlation of the observed and calculated gravity and magnetic anomalies:

- the models strongly suggest an anomalously dense mantle towards the oceanic domain;
- Moho shows a general deepening trend from the marginal highs towards the continent, with anomalous shallowing and crustal thinning pattern beneath the Møre Marginal High;
- the volcanics incorporated in the sedimentary sequence with some extension towards the basin are required. Magnetic data on the marginal highs are difficult to interpret, most likely due to the presence of the complex sequences of extrusives. The fit was obtained by changing the geometry and magnetic properties of the flood basalt layer, i.e., the lava body was subdivided into some blocks and different magnetic properties were assigned;
- a high-density body in the lower continental crust beneath the Halten Terrace along the Geoseismic Transect BB' is suggested, to account for the observed high magnetic and density anomalies in the area;

- an anomalously high velocity body (LCB) is strongly suggested beneath the Vøring Marginal High, with some extension towards the basin. Still, the presence of the LCB beneath the Møre Marginal High is much more uncertain;
- the variation of properties within the layers has been tested. After increasing density of the sediments due to compaction in the deep Rås Basin and the basin between the Helland-Hansen and Modgunn Arch, the gravity response was approximated the observed anomaly. The remaining slight misfit on both profiles might be a result of density variations along the margin and off line.

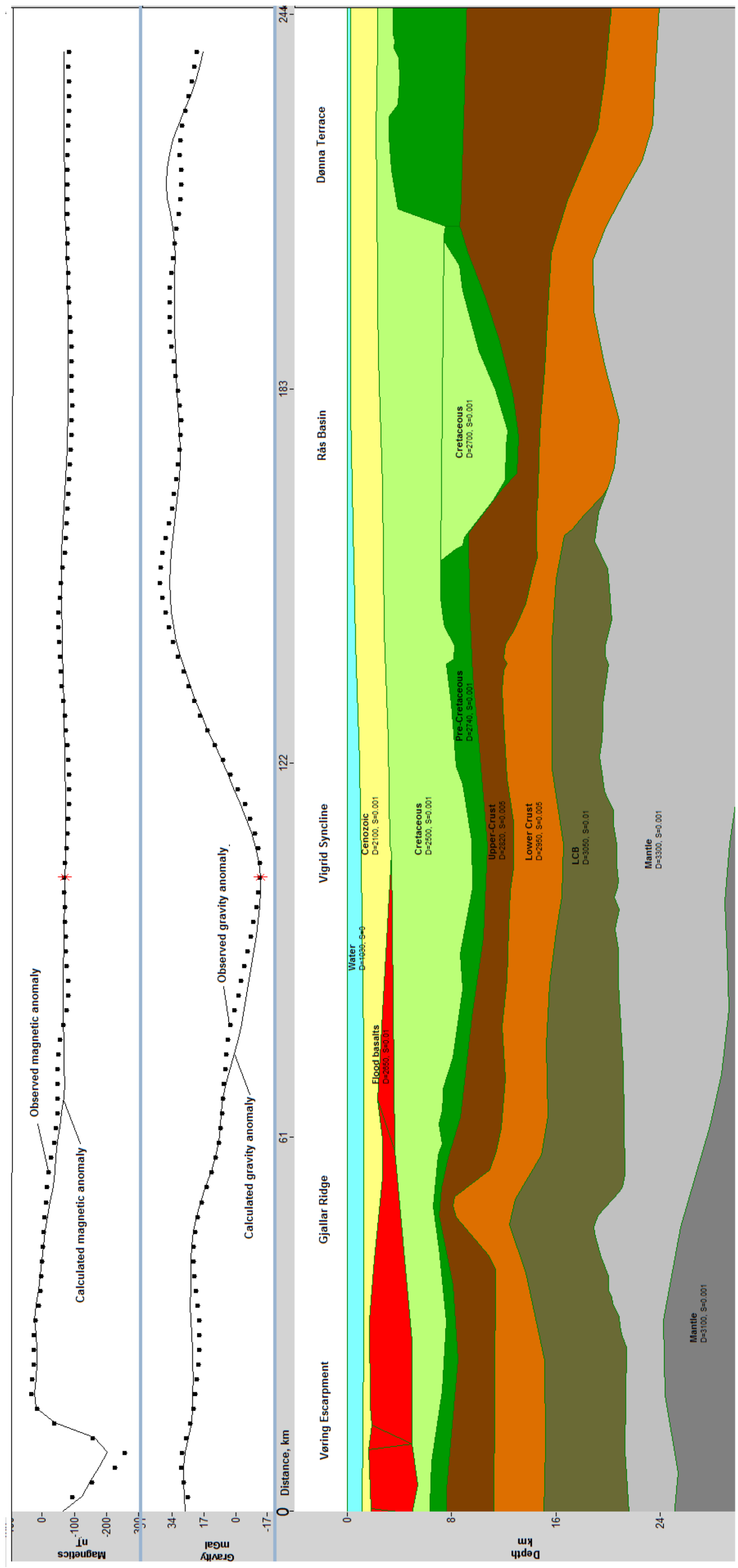

Figure 6.9: 2D model for the Geoseismic Transect AA’. The inferred petrophysical properties are indicated with densities (D) in kg/m3 and susceptibilities (S) SI. See Fig.4.1 - 4.4 for the Transect location.

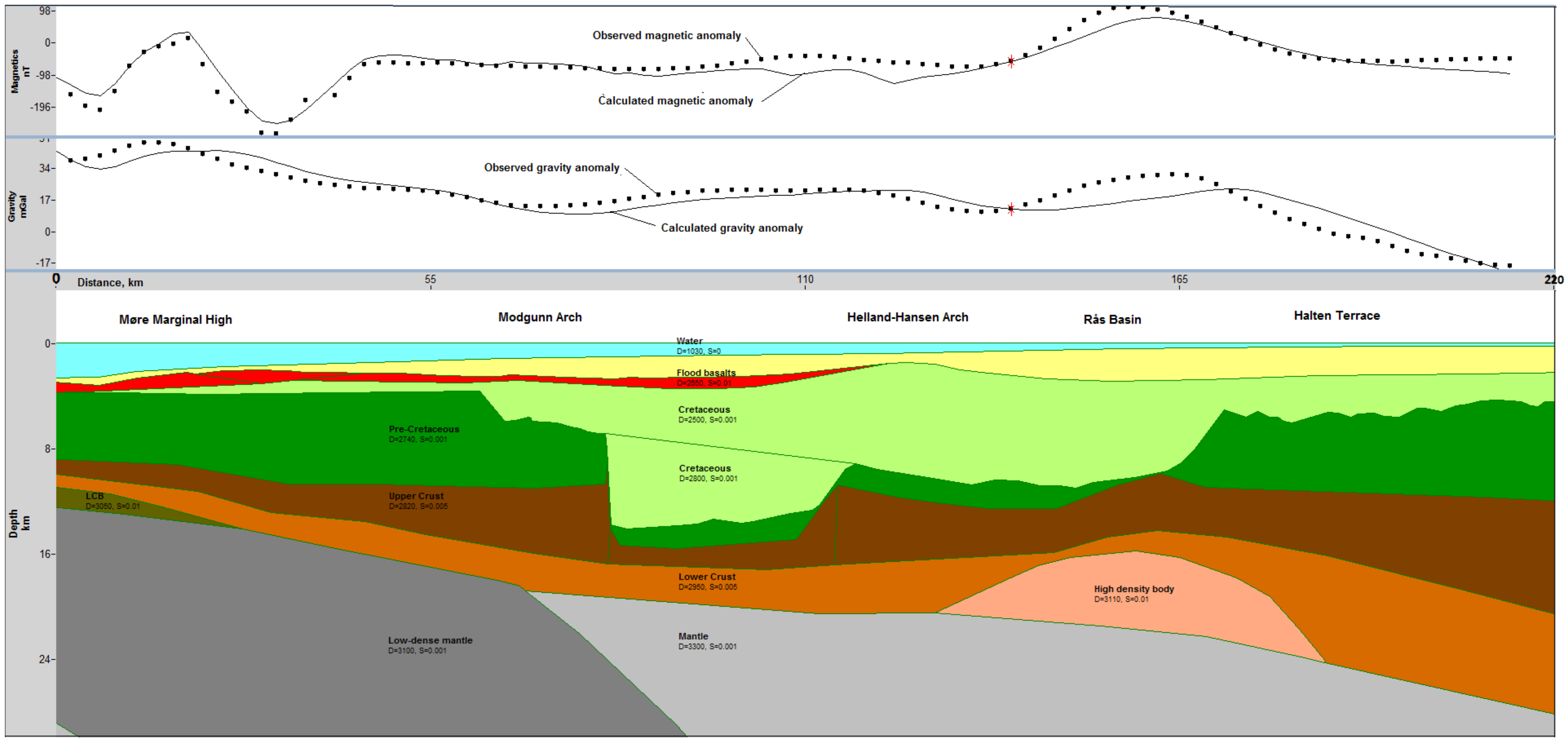

Figure 6.10: 2D model for the Geoseismic Transect BB'. The inferred petrophysical properties are indicated with densities (D) in kg/m3 and susceptibilities (S) SI. See Fig.4.1 - 4.4 for the Transect location.

7 Conclusion

Integration of seismic data with potential field data enabled to construct crustal transects across the Vøring and Møre rifted margins. 2D crustal models were constructed by forward gravity and magnetic modeling on the basis of the regional geological context, available reflection and refraction data and the information from previous studies.

The geometrical crustal structure obtained from seismic data provides a good insight into the main features of the margin. However, a considerable uncertainty exists with respect to the deep interfaces, and especially in detecting sub-basaltic basement structures, where intrusions and lava flows can perturb the imaging of the underlying basement. To resolve that complication on a regional scale, it is fundamental to combine various types of dataset and lead a multi-method integrated study. The geometry of each body in the model has to be tied to as many constraints as possible (e.g. seismic horizons, wells), with necessary higher resolution dataset, deep sea drilling and sampling information.

Gravity and magnetic data provide suitable information for regional structural mapping and can significantly improve the seismic interpretation, especially with understanding of the deep structures and in the areas with volcanics. The seismic data set alone is not conclusive, and in order to correctly constrain the deep geometries across the Vøring and Møre rifted margins, it is important to combine the seismic dataset with the gravity and magnetic field data, together with the geological approach.

Bibliography

Allen, P.A., Allen, J.R., 2005. *Basin analysis: principles and applications*. Blackwell publishing, 2 ed.

Andersen, T.B., Jamtveit, B., 1990. *Uplift of deep crust during orogenic extensional collapse: A model based on field studies in the Sogn-Sunnfjord Region of western Norway*, Tectonics, 9, 1097-1111.

Andersen, T.B., Osmundsen, P.T., Jolivet, L., 1994. *Deep crustal fabrics and a model for the extensional collapse of the southwest Norwegian Caledonides*, Journal of Structural Geology, 16, 1191-1203.

Andersen, O.B., Knudsen, P., Berry, P., Kenyon, S., 2008. *The DNSC08 ocean wide altimetry derived gravity field*, Presented to EGU-2008, Vienna, Austria, April, 2008.

Berndt, C., Planke, S., Alvestad, E., Tsikalas, F., Rasmussen, T., 2001. *Seismic volcanostratigraphy of the Norwegian Margin: constraints on tectonomagmatic break-up processes*, Journal of the Geological Society, 158, 413-426.

Blystad, P., Brekke, H., Faerseth, R.B., Larsen, B.T., Skogseid, J., Tørrudbakken, B., 1995. *Structural elements of the Norwegian continental margin*, Norwegian Petroleum Directorate, Bulletin 8.

Boilot, G., Grimaud, S., Mauffret, A., Mougenot, D., Kornprobst, J., Mergoil-Daniel, J., Torrent, G., 1980. *Ocean-continent boundary off the Iberia margin: a serpentinite diapir west of the Galicia Bank*, Earth and Planetary Science Letters, 48, 23-34.

Boilot, G., Winterer, E.L., Meyer, A.W., and al., e., 1987a. *Introduction, objectives, and proncipal results: Ocean Drilling Program Leg 103, West Galicia Margin*, in Proceedings of the Ocean Drilling Program, 3-17.

Boilot, G., Winterer. E.L., Recq, M., Girardeau, J., Kornprobst, J., Loreau, J.P., Malod, J., Mougenot, D., 1987b. *Tectonic denudation of upper mantle along passive margins- a model based on drilling (ODP Leg 103) and diving (Gallunate Cruise) results, western Galicia margin, Spain*, AAPG Bulletin American Association of Petroleum Geologists, 71, 531-531.

Breivik, A.J., Mjelde, R., Raum, T., Faleide, J.I., Murai, Y., Flueh, E.R., 2011. *Crustal structure beneath the Trøndelag Platform and adjacent areas of the mid-Norwegian margin, as derived from wide-angle seismic and potential field data*, Norwegian Journal of Geology, 90, 141-161.

Brekke, H., 2000. *The tectonic evolution of the Norwegian Sea Continental Margin with emphasis on the Vøring and Møre Basins*, in Dynamics of the Norwegian Margin, 167, 327-378, Published for the Geological Society by Blackwell, Oxford.

Brekke, H., Sjulstad, H.I., Magnus, C., Williams, R.W., 2001. *Sedimentary environments offshore Norway - an overview*, in Sedimentary environments offshore Norway - Palaeozoic to Recent, 10, 7-37, eds. Martinsen, O.J. and Dreyer, T., Elsevier Science B.V., Amsterdam.

Buck, W.R., 1991. *Modes of continental lithospheric extension*, Journal of Geophysical Research, 96, 21161-41339.

Davis, G.H., 1980. *Structural characteristics of metamorphic core complexes, southern Arizona*, in Cordilleran Metamorphic Core Complexes, Memoir, 35-77, eds. Crittenden, M.J., Coney, P., Davis, G.H., Geological Society of America, Boulder, CO, United States.

Davis., M., Kusznir, N., 2004. *Depth-Dependent Lithospheric Stretching at Rifted Continental Margins*, in Proceedings of NSF Riftet margins Theoretical Institute, 92-136, ed. Karner, G.D., Columbia University Press.

Ebbing, J., Lundin, E., Olesen, O., Hansen, E., K., 2006. *The mid-Norwegian margin: A discussion of crustal lineaments, mafic intrusions, and remnants of the Caledonian root by 3D density modelling and structural interpretation*, Journal of Geological Society, London, 163, 47-60.

Eldholm, O., Thiede, J., Taylor, B., 1989. *Evolution of the Vøring volcanic margin*, in Proceedings of the Ocean Drilling Program, Scientific Results, 104, 1033-1065, eds. Eldholm, O., Thiede, J., Taylor, E. College Sation, TX (Ocean Drilling Program).

Faerseth, R., B., Lien, T., 2002. *Cretaceous evolution in the Norwegian Sea - a period characterized by tectonic quiescence*, Marine and Petroleum Geology, 19, 1005-1027.

Froitzheim, N., Manatschal, G., 1996. *Kinematics of Jurassic rifting, mantle exhumation, and passive margin formation in the Austroalpine and Penninic nappes (eastern Switzerland)*, Geological Society of America Bulletin, 108, 1120-1133.

Gernigon, L., Ringenbach, J., C., Planke, S., Le Gall, B., Jonquet-Kolstø, H., 2003. *Extension, crustal structure and magmatism at the outer Vøring Basin, Norwegian margin*, Journal of the Geological Society, London, 160, 197-208.

Gernigon, L., Ringenbach, J., C., Planke, S., Le Gall, B., 2004. *Deep structures and break-up along volcanic rifted margins: insights from intergated studies along the outer Vøring Basin (Norway)*, Marine and Petroleum Geology, 21, 363-372.

Gernigon, L., Olesen, O., Ebbing, J., Wienecke, S., Gaina, C., Mogaard, J., O., Sand, M., Myklebust, R., 2009. *Geophysical insights and early spreading history in the vicinity of the Jan Mayen Fracture Zone, Norwegian-Greenland Sea*, Tectonophysics, 468, 185-205.

Gernigon, L., Lucazeau, F., Brigaud, F., Ringenbach, J.C., Planke, S., Gall, B., 2006. *A moderate melting model for the Vøring margin (Norway) based on structural observations and a thermo-kinematical modelling: Implication for the meaning of the lower crustal bodies*, Tectonophysics, 412, 255-278.

Gradstein, F.M., Ogg, J.G., Smith, A. et al., 2004. *A Geologic Time Scale 2004*, Cambridge University Press.

Group-Galice, 1979. *The continental margin off Galicia and Portugal: acoustical stratigraphy, dredge stratigraphy, and structural evolution*, in Proceedings of the Deep Sea Drilling Program, 633-662.

Hagevang, T., Eldholm, O., Aalstad, I., 1983. *Pre-23 magnetic anomalies between Jan Mayen and Greenland Senja fracture zones in the Norwegian Sea*, Marine Geophysical Research, 5, 345-363.

Hartz, E.H., Andresen, A., 1997. *From collision to collapse: Complex strain permutations in the hinterland of the Scandinavian Caledonides*, Journal of Geophysical Research, 102, 697-711.

Huismans, R., Beaumont, C., 2011. *Depth-dependent extension, two-stage breakup and cratonic underplating at rifted margins*, Nature, 473, 74-78.

Huismans, R.S., Beaumont, C., 2008. *Complex rifted continental margins explained by dynamical models of depth-dependent lithospheric extension*, Geology, 36, 163-166.

Jackson, J.A., McKenzie, D.P., 1983. *The geometrical evolution of normal fault systems*, J. Struct. Geol., 5, 471-482.

Kusznir, N.J., Karner, G.D., Egan, S.S., 1987. *Geometric, thermal and isostatic consequences of detachments in continental lithosphere extension and basin formation*, in Sedimentary Basins and Basin Forming Mechanisms, 12, 185-203, eds. Beaumont, C., Tankard, A. J. Can. Sot. Pet. Geol. Mem.

Kusznir, N.J., Ziegler, P.A., 1992. *The Mechanics of Continental Extension and Sedimentary Basin Formation - a Simple-Shear Pure-Shear Flexural Cantilever Model*, Tectonophysics, 215, 117-131.

Lavier, L.L., Manatschal, G., 2006. A mechanism to thin the continental lithosphere at magma-poor margins, Nature, 440, 324-328.

Laxon, S., McAdoo, D., 1994. *Arctic Ocean gravity field derived from ERS-1 satellite altimetry*, Science, 256, 621-624.

Le Pichon, X., Sibuet, J.C., 1981. *Passive Margins: A Model of Formation*, JGR, 86, 3708-3720.

Lemoine, M., Tricart, P., Boillot, G., 1987. *Ultramafic and gabbroic ocean-floor of the Ligurian Tethys (alps, Corsica, Apennines) - in search of a genetic model*, Geology, 15, 622-625.

Lister, G.S., Etheridge, M.A., Symonds, P.A., 1986. *Detachment faulting and the evolution of passive continental margins*, Geology, 14, 246-250.

Lister, G.S., Etheridge, M.A., Symonds, P.A., 1991. *Detachment models for the formation of passive continental margins*, Tectonics, 10, 5, 1038-1064.

Lundin, E.R., Dore, A.G., 1997. *A Tectonic model for the Norwegian passive margin with implications for the NE Atlantic Early Cretaceous to break-up*, Journal of the Geological Society, London, 154, 545-550.

Lundin, E.R., Dore, A.G., 2002. *Mid-Cenozoic post-breakup deformation in the 'passive' margins bordering the Norwegian-Greenland Sea*, Marine and Petroleum Geology, 19, 79-93.

Manatschal, G., 2004. *New models for evolution of magma-poor rifted margins based on a review of data and concepts from West Iberia and the Alps*, Int J Earth Sci, 93, 432-466.

Maystrenko, Y., Scheck-Wenderoth, M., 2009. *Density contrasts in the upper mantle and lower crust across the continent-ocean transition: constraints from 3-D gravity modelling at the Norwegian margin*, GJI, 179, 536-548.

Mauring, E., Kihle, O., 2006. *Leveling aerogeophysical data using a moving differential median filter*, Geophysics, 71, L5-L11.

McKenzie, D., 1978. *Some remarks on the development of sedimentary basins*, Earth Planet Sci Lett, 40, 25-32.

Meyer, R., Wijk, J., Gernigon, L., 2007. *The North Atlantic Igneous Province: A review of models for its formation*, Geological Society of America, 430, 525-552.

Mjelde, R., Kasahara, J., Shimamura, H., Kamimura, A., Kanazawa, T., Kodaira, S., Raum, T., Shiobara, H., 2002. *Lower crustal seismic velocity-anomalies; magmatic underplating or serpentinized peridotite? Evidence from the Vøring Margin, NE Atlantic*, Marine Geophysical Research, 23, 169-183.

Mjelde, R., Shimamura, H., Kanazawa, T., Kodaira, S., Raum, T., Shiobara, H., 2003. *Crustal lineaments, distribution of lower crustal intrusives and structural evolution of the Vøring Margin, NE Atlantic; nw insights from wide-angle seismic models*, Tectonophysics, 369, 199-218.

Mjelde, R., Faleide, J., I., Breivik, A., J., Raum, T., 2008. *Lower crustal composition and crustal lineaments on the Vøring Margin, NE Atlantic: A review*, Tectonophysics, 472, 183-193.

Mjelde, R., Raum, T., Kandilarov, A., Murai, Y., Takanami, T., 2008. *Crustal structure and evolution of the outer Møre Margin, NE Atlantic*, Tectonophysics, 468, 224-243.

Mosar, J., Eide, E.A., Osmundsen, P., T., Sommaruga, A., Torsvik, T.,H., 2002. *Greenland - Norway separation: A geodynamic model for the North Atlantic*, Norwegian Journal of Geology, 82, 281-298.

Nagel, T.J., Buck, W.R., 2004. *Symmetric alternative to asymmetric rifting models*, Geology, 32, 937-940.

Nagel, T.J., Buck, W.R., 2007. *Control of rheological stratification on rifting geometry: a symmetric model resolving the upper plate paradox*, International Journal of Earth Sciences, 96, 1047-1057.

Olesen, O., Bronner, M., Ebbing, J., Gellein, J., Gernigon, L., Koziel, J., Lauritsen, T., Myklebust, R., Pascal, C., Sand, M., Solheim, D., Usov, S., 2010a. *New aeromagnetic and gravity compilations from Norway and adjacent areas: methods and applications*, In: Vining, B.A. and Pickering, S.C. (eds.) Petroleum Geology: From mature basins to new frontiers. Proceedings of the 7th Petroleum Geology Conference. Geological Society of London, 7, 559-586.

Olesen, O., Ebbing, J., Gellein, J., Kihle, O., Myklebust, R., Sand, M., Skilbrei, J.S., Solheim, D., Usov, S., 2010b. *Gravity anomaly map Norway and adjacent areas*, Scale 1:3 million, Geological Survey of Norway, Trondheim.

Osmundsen, P., T., Sommaruga, A., Skilbrei, J., R., Olesen, O., 2002. *Deep structure of the Mid Norway rifted margin*, Norwegian Journal of Geology, 82, 205-224.

Osmundsen, O., T., Ebbing, J., 2008. *Styles of extension offshore mid-Norway and implications for mechanisms of crustal thinning at passive margins*, Tectonics, 27, TC6016.

Peron-Pindivic, G., Manatschal, G., Osmundsen, P., T., in press. *Similarities and differences between key Atlantic margins: a review of observations and concepts*, in press for Marine and Petroleum Geology (Invited).

Peron-Pindivic, G., Manatschal, G., 2009. *The final rifting evolution at deep magma-poor passive margins from Iberia-Newfoundland: a new point of view*, Int J Earth Sci, 98, 7, 1581-1597.

Peron-Pindivic, G., Manatschal, G., Minshull, T.A., Sawyer, D.S., 2007. *Tectonosedimentary evolution of the deep Iberia-Newfoundland margins: Evidence for a complex breakup history*, Tectonics, 26, 1-19.

Peron-Pindivic, G., Gernigon, L., Gaina, C., Ball, P., in press. *Insights from the Jan-Mayen system in the Norwegian-Greenland Sea - I: mapping of a microcontinent*, in press for Geophysical Journal International.

Peron-Pindivic, G., Gernigon, L., Gaina, C., Ball, P., in press. *Insights from the Jan-Mayen system in the Norwegian-Greenland Sea - II: architecture of a microcontinent*, in press for Geophysical Journal International.

Planke, S., Symonds, P.A., Alvestad, E., Skogseid, J., 2000. *Seismic volcanostratigraphy of large-volume basaltic extrusive complexes on rifted margins*, Journal of Geophysical Research, 105, 19335-19351.

Planke, S., Rasmussen, T., Rey, S.S., Myklebust, R., 2005. *Seismic characteristics and distribution of volcanic intrusions and hydrothermal vent complexes in the Vøring and Møre basins*, in Petroleum Geology: North-West Europe and Global Perspectives - Proceedings of the 6th Petroleum Geology Conference, ed. Dore, A.G.V.B. Geological Society London, 833-844.

Raum, T., Mjelde, R., Digranes, P., Shimamura, H., Shiobara, H., Kodaira, S., Haatvedt, G., Sørenes, N., Thorbjørnsen, T., 2002. *Crustal structure of the southern part of the Vøring Basin, mid-Norway margin, from wide-angle seismic and gravity data*, Tectonophysics, 355, 99-126.

Raum., T., Mjelde, R., Shimamura, H., Murai, Y., Braastein, E., Karpuz, R.M., Kravik, K., Kostoe, H.J., 2006. *Crustal structure and evolution of the southern Vøring Basin and Vøring Transform Margin, NE Atlantic*, Tectonophysics, 415, 167-202.

Reston, T.J., 2005. *Polyphase faulting during the development of the west Galicia rifted margin*, Earth and Planetary Science Letters, 237, 561-576.

Reston, T.J., 2009. *The structure, evolution and symmetry of the magma-poor rifted margins of the North and Central Atlanti A synthesis*, Tectonophysics, 468, 6-27.

Reston, T.J., Krawczyk, C.M., Klaeschen, D., 1996. *The S reflector west of Galicia (Spain): Evidence from prestack depth migration for detachment faulting during continental breakup*, Journal of Geophysical Research-Solid Earth, 101, 8075-8091.

Roberts, D., 2003. *The Scandinavian Caledonides: event chronology, palaeogeographic settings and likely modern analogues*, Tectonophysics, 365, 283-299.

Ruppel, C., 1995. *Extensional processes in continental lithosphere*, Journal of Geophysical Research-Solid Earth, 100, 24187-24215.

Sandwell, D.T., Smith, W.H.F., 1997. *Marine gravity anomaly from Geosat and ERS 1 satellite altimetry*, Journal of Geophysical Research-Solid Earth, 102, 10039-10054.

Sawyer, D., Whitmarsh, R.B., Klaus, A. and al., e., 1994. *Introduction. in Proceedings of the Ocean Drilling Program*, 5-10.

Sawyer, D.S., Coffin, M.F., Reston, T.J., Stock, J.M., Hopper, J.R., 2007. *COBBOOM: The Continental Breakup and Birth of Oceans Mission*, Scientific Drilling, 13-25.

Scott, R.A., Ramsey, L.A., Jones, S.M., Sinclair, S., Pickles, C.S., 2005. *Development of the Jan Mayen microcontinent by linked propagation and retreat of spreading ridges*, in Onshore-Offshore relationships on the North Atlantic Margin, 69-82, eds. Wandaas, B.T.G., Nystuen, J.P., Eide, E., Gradstein, F. Norwegian Petroleum Society (NPF), Special Publication.

Skogseid, J., Planke, S., Faleide, J.I., Pedersen, T., Eldholm, O., Neverdal, F., 2000.*NE Atlantic continental rifting and volcanic margin formation*, in Dynamics of the Norwegian margin, 167, 295-326, published for the Geological Society by Blackwell, Oxford.

Skogseid, J.,Eldholm, O., 1987.*Early Cenozoic crust at the Norwegian continental margin and the conjugate Jan Mayen Ridge*, Journal of Geophysical Research, 92, 11471-11491.

Skogseid, J., Pedersen, T., Eldholm, O., Larsen, B.T., 1992.*Tectonism and magmatism during NE Atlantic continental break-up: the Vøring basin*, in Magmatism and the Causes of Continental Break-up, 305-320, eds. Storey, B.C., Alabaster, T., Plankhurst, R.J., Geological Society, London, Special Publications.

Tucholke, B.E., Sibuet, J.C., Klaus, A. and al., e., 2004. *Leg 210 summary*, in Proceedings of the Ocean Drilling Program.

Wernicke, B., 1985. *Uniform-sense normal simple shear of the continental lithosphere*, Can. J. Earth Sci. 22, 108-125.

White, N., 1990. *Does the uniform stretching model work in the North Sea?*, in Tectonic Evolution of the North Sea Rifts, International Lithosphere Program Publication, 181, 217-239, eds. Blundell, D. J., Gibbs, A. D.

White, N.J., Jackson, J.A., McKenzie, D.P., 1986. *The relationship between the geometry of normal faults and that of the sedimentary layers in their hanging-walls*, Journal of Structural Geology, 8, 897-909.

White, R., McKenzie, D., 1989. *Magmatism at rift zones: the generation of volcanic continental margins and flood basalts*, Journal of Geophysical Research, 94 (B6), 7685-7729.

Whitmarsh, R.B., Beslier, M.O., Wallace, P.J., et al., 1998. *Leg 173 Introduction*, in Proceedings of the Ocean Drilling Program.

Whitmarsh, R.B., Manatschal, G., Minshull, T.A., 2001. *Evolution of magma-poor continental margins from rifting to seafloor spreading*, Nature, 413, 150-154.

Van Wijk, J.W., Meer, R., Cloetingh, S.A.P.L, 2004. *Crustal thickening in an extensional regime: application to the mid-Norwegian Vøring margin*, Tectonophysics, 387, 217-228.

Ziegler, P.A., 1983. *Comment on: Crustal thinning and subsidence in the North Sea*, Nature, 304, 561.

Ziegler, P.A., 1988. *Evolution of the Arctic-North Atlantic and the Western Tethys*, American Association of Petroleum Geologists, Tulsa, Okla, 43.